IV. 研究成果の刊行物・別刷

BRAIN RESEARCH 1250 (2009) 232–241

available at www.sciencedirect.com

ScienceDirect

www.elsevier.com/locate/brainres

BRAIN RESEARCH

Research Report

Motor impairment and aberrant production of neurochemicals in human α-synuclein A30P+A53T transgenic mice with α-synuclein pathology☆

Masaki Ikeda[a], Takeshi Kawarabayashi[b], Yasuo Harigaya[d], Atsushi Sasaki[c], Shuichi Yamada[g], Etsuro Matsubara[e], Tetsuro Murakami[f], Yuya Tanaka[f], Tomoko Kurata[f], Xu Wuhua[f], Kenji Ueda[h], Hisashi Kuribara[i], Yasushi Ikarashi[j], Yoichi Nakazato[c], Koichi Okamoto[a], Koji Abe[f], Mikio Shoji[b,]*

[a]*Department of Neurology, Gunma University Graduate School of Medicine, Maebashi, Japan*
[b]*Department of Neurology, Hirosaki University School of Medicine, Hirosaki, Japan*
[c]*Department of Human Pathology, Gunma University Graduate School of Medicine, Maebashi, Japan*
[d]*Department of Neurology, Maebashi Red Cross Hospital, Maebashi, Gunma, Japan*
[e]*Department of Alzheimer's Disease Research, National Institute for Longevity Sciences, Obu, Japan*
[f]*Department of Neurology, Neuroscience, Biophysiological Science, Okayama University Graduate School of Medicine and Dentistry, Okayama, Japan*
[g]*Immuno-Biological Laboratories Co., Ltd., Mikasa, Hokkaidio, Japan*
[h]*Department of Neural Plasticity, Tokyo Institute of Psychiatry, Setagaya-ku, Tokyo, Japan*
[i]*Tokyo University of Social Welfare, Isesaki, Japan*
[j]*R and D Division, Tsumura and Co., Ltd, Inashiki, Japan*

ARTICLE INFO

Article history:
Accepted 6 October 2008
Available online 1 November 2008

Keywords:
α-synuclein
Mutation
Transgenic mouse
Parkinson's disease
Neurochemical

ABSTRACT

Missense point mutations, duplication and triplication in the α-synuclein (αSYN) gene have been identified in familial Parkinson's disease (PD). Familial and sporadic PD show common pathological features of αSYN pathologies, e.g., Lewy bodies (LBs) and Lewy neurites (LNs), and a loss of dopaminergic neurons in the substantia nigra that leads to motor disturbances. To elucidate the mechanism of αSYN pathologies, we generated TgαSYN transgenic mice overexpressing human αSYN with double mutations in A30P and A53T. Human αSYN accumulated widely in neurons, processes and aberrant neuronal inclusion bodies. Sarcosyl-insoluble αSYN, as well as phosphorylated, ubiquitinated and nitrated αSYN, was accumulated in the brains. Significantly decreased levels of dopamine (DA) were recognized in the striatum. Motor impairment was revealed in a rotarod test. Thus, TgαSYN is a useful model for analyzing the pathological cascade from aggregated αSYN to motor disturbance, and may be useful for drug trials.

☆ Grant numbers and sources of supports: Supported by **Grant-in-Aid for** Grants-in-Aid for Primary Amyloidosis Research Committee (M. S.), from the Ministry of Health, Labor and Welfare of Japan and by Grants-in-Aid for Scientific Research (B) (M.S.: 19390233, K.A.: 18390257), (C) (M.I.: 19590980, T.K.: 19590976, A.S.: 18500276, E.M.: 18590968), from the Ministry of Education, Culture, Sports, Science and Technology, Japan.

* *Corresponding author.* Fax: +81 172 39 5143.
E-mail address: mshoji@hirosaki-u.ac.jp (M. Shoji).

0006-8993/$ – see front matter © 2008 Published by Elsevier B.V.
doi:10.1016/j.brainres.2008.10.011

1. Introduction

αSYN was originally isolated from senile plaques in Alzheimer's disease as a protein of 35 highly hydrophobic amino acid metabolites, known as the non-amyloid component (NAC), derived from a 140 amino-acid precursor encoded by a gene on chromosome 4 (Ueda et al., 1992; Chen et al., 1995), which has homology to rat and Torpedo αSYN and songbird synelfin (George et al., 1995). αSYN is highly abundant in presynaptic terminals (Iwai et al., 1995) and has potential roles in synaptic function and neural plasticity (George et al., 1995; Clayton and George, 1998).αSYN binds to phospholipid vesicles and inhibits PLD2, a regulator of vesicle membrane budding (Liscovitch et al., 2000; Lotharius and Brundin, 2000; Payton et al., 2000), and also plays modulatory roles in the release of dopamine vesicles (Abeliovich et al., 2000).

A few cases of familial Parkinson's disease (FPD) have been linked to missense point mutations in αSYN with A53T (Polymeropoulos et al., 1997), A30P (Kruger et al., 1998) and E46K (PARK1) (Zarranz et al., 2004). Soon after the first A53T missense mutation of αSYN was discovered, the main component of Lewy bodies (LBs) was identified as insoluble aggregates of αSYN (Baba et al., 1998). αSYN and phosphorylated-Ser129 αSYN accumulated in LBs and Lewy neurites (LNs) in PD and Dementia with Lewy bodies (DLB) (Fujiwara et al., 2002; Hasegawa et al., 2002). Then, a second causative gene known as *parkin* (Kitada et al., 1998) was found in familial autosomal recessive juvenile Parkinson's disease (PARK2). *Parkin* ubiquitinates αSYN normally and this process is aberrantly altered in PD (Shimura et al., 2001). Acceleration of oligomerization or protofibrillization is a common property of mutant αSYN (Conway et al., 2001; Choi et al., 2004). Recently, triplication of the αSYN locus (PARK4) was identified in an "Iowanian kindred" with autosomal dominant Lewy body disease (Singleton et al., 2002). Subsequently, duplication of the αSYN gene locus was also reported as a cause of familial PD (Chartier-Harlin et al., 2004). These findings suggest that overexpression of wild type αSYN also leads to facilitation of insoluble aggregation of αSYN. α-synucleinopathy is a disease entity which shares common pathological accumulation of insoluble aggregates of αSYN in the neurons and processes of PD, DLB, Hallervorden–Spatz disease, pure autonomic failure and in the glial cells of multiple system atrophy (MSA) (Goedert, 2000; Hardy and Gwinn-Hardy, 1998; Spillantini et al., 1997; Tu et al., 1998; Galvin et al., 2000; Shoji et al., 2000; Arai et al., 2000).

To elucidate the pathological mechanism of LBs and LNs associated with the decrease in dopamine (DA) production, it is necessary to investigate the aberrant mechanism of mutant αSYN, which is an essential molecule consisting of LBs and LNs (Baba et al., 1998). Here, we generated transgenic (Tg) mice expressing human mutant αSYN A30P+A53T under a human Thy-1 promoter, named as TgαSYN. Overexpression of double mutant human αSYN was expected to lead to further synergistic effects and induce severe α-synucleinopathies and neurodegeneration (Citron et al., 1998; Chishti et al., 2001). TgαSYN showed significant motor impairment in rotarod test, accumulation of insoluble αSYN, aberrant inclusions and decreased dopamine levels. These findings indicate that TgαSYN is a useful animal model to investigate the crucial pathogenesis of α-synucleinopathies, and it may help to develop therapeutic agents.

2. Results

2.1. *Expression of αSYN in transgenic mice and analyses of RT-PCR*

We used the transgene construct hThy1-αSYN A30P+A53T to generate transgenic (Tg) mice, TgαSYN (Fig. 1a). PCR analysis of tail-derived DNA revealed 18 positive Tg mice for human αSYN and EGFP among 129 F0 mice. Five of the 18 Tg mice showed the strongest green fluorescence under irradiation at 365 nm ultraviolet (Fig. 1b). These selected independent lines (#8707, #8713, #8718, #8812, #8819) were mated with BDF1 mice and raised for examination. The following Tg mice were analyzed: 18 positive Tg progenies, 60 F1 Tg (#8707: 2, #8713: 31, #8718: 5, #8812: 10, #8819: 12) and 135 F2 Tg (#8707: 0, #8713: 101, #8718: 2, #8812: 29, #8819: 3). The mRNA expressions of human αSYN A30P+A53T and EGFP in TgαSYN brains were confirmed by RT-PCR, showing the same expression levels of human αSYN A30P+A53T and EGFP at three, eight and 17 months old, respectively (Figs. 1c and d). Western blot using LB509 recognized a 16 kD band corresponding to human αSYN only in Tg mice. AB5038 recognized a 16 kD band corresponding to both human and mouse αSYN. The expression level of human αSYN was 130% of that of endogenous mouse αSYN (Fig. 1e).

2.2. *Histological studies*

Immunocytochemistry of sagittal sections of a seven-month-old #8707 TgαSYN brain by LB509 revealed extensive human αSYN immunostaining in the brainstem, hippocampus, thalamus, cerebral cortex and cerebellum (Fig. 2a, arrow indicates the substantia nigra), but no staining in the non-Tg mouse (Fig. 2b). The TgαSYN brain showed atrophy of the cerebral cortex and cerebellum (Fig. 2a). The HE stain showed eosinophilic inclusion bodies and vacuoles in the cytoplasm of neurons in the substantia nigra (Fig. 2c, arrow), and in the dentate nucleus of TgαSYN (Fig. 2h, arrow). These cytoplasmic inclusions were stained with human-αSYN specific antibody, LB509 (Fig. 2d, arrow, and Fig. 2i, arrow), and anti-αSYN antibody, 42/α-Synuclein (Fig. 2j, arrows). Nitrated α/β synuclein was also stained in the cytoplasmic inclusions (Fig. 2e, arrow,). Ubiquitin-positive inclusions were observed in neurons at brainstem (Fig. 2f, arrow), and dystrophic neurites in the dentate nucleus of TgαSYN (Fig. 2g). Staining of phosphorylated synuclein showed diffuse staining in somatodendrites of TgαSYN neurons (Fig. 2k). Gallyas–Braak staining revealed dystrophic neurites in the dentate nucleus of TgαSYN (Fig. 2l) in ubiquitin-positive structures in the same region (Fig. 2g). Anti-tyrosine hydroxylase (TH) immuno-positive neurons in the locus ceruleus showed weak immunostaining intensity in TgαSYN (Fig. 2m), compared with those of non-Tg mice brains (Fig. 2n). The intensity of substance P immunopositive synapses in the striata of TgαSYN brains (Fig. 2o) was weaker than that of non-Tg mice brains (Fig. 2p). Severe astrocytosis

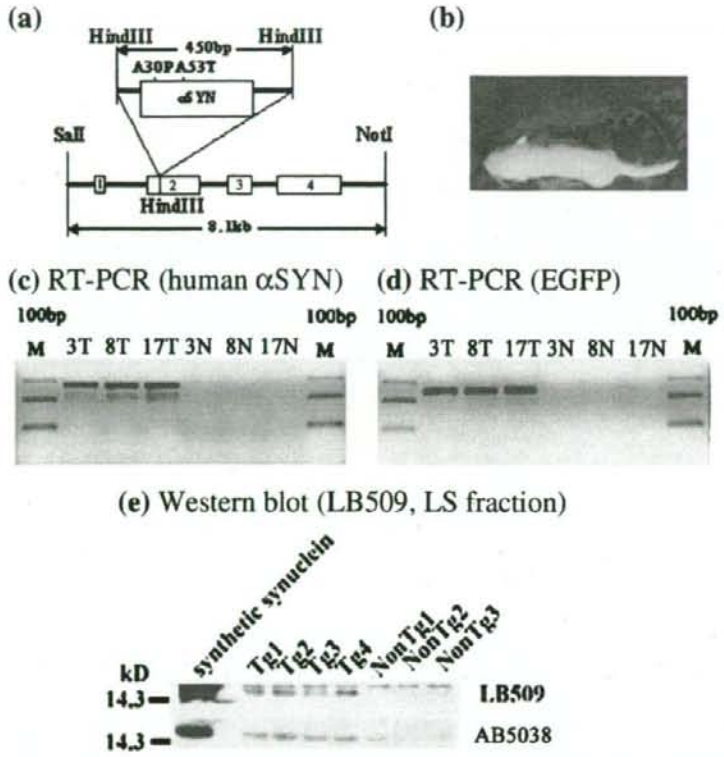

Fig. 1 – The mutant αSYN A30P+A53T construct and the expression of EGFP. (a) The structure of the construct: hThy1-αSYN A30P+A53T. (b) TgαSYN (#8713) showed fluorescence by EGFP (enhanced green fluorescence protein) under 365 nm long wave UV (EGFP-negative non-Tg mouse in the upper location, EGFP-positive Tg mouse in the lower location). (c) Analyses of RT-PCR transcripts: Human αSYN mRNA transcripts (exons 2–4) were detected as 280 bp in TgαSYN brains, but not in non-Tg mice brains, and the intensity of PCR products was the same level as three-, eight-, and 17-month-old Tg mice brains. (d) EGFP mRNA transcripts were detected in TgαSYN brains at the same level at three, eight and 17 months of age, but not in non-Tg mice brains (N showed non-Tg mice brains, T showed Tg mice brains). (e) The expression of human αSYN was detected as a 16 kD band at the same size as recombinant synthetic αSYN by Western blot using LB509 in LS-soluble fractions of TgαSYN #8713 (Tg1–4) mice brains, but not in three 14-month-old non-Tg mice brains (upper lane). AB5038 recognized a 16 kD band corresponding to human and mouse αSYN (lower lane). The expression level of human αSYN was about 130% of that of endogenous mouse αSYN. Synthetic αSYN (SS) was used as a marker of 16 kD αSYN (BIOMOL Research Laboratories Inc., Plymouth Meeting, PA).

was observed in the cerebellum of a 16-month-old TgαSYN (Fig. 2q). An EM study demonstrated cytoplasmic inclusions (Fig. 2r, arrow) and intranuclear inclusions (Fig. 2s, arrows) in the neurons of the brainstem. These inclusion bodies lacked the typical halo and fibrillar structure of LBs.

2.3. *Western blot analysis*

Fourteen-month-old TgαSYN showed a 16 kD band corresponding to αSYN in the LS-soluble fraction (L), Triton-soluble fraction (T), sarcosyl-soluble (S) and sarcosyl-insoluble fractions (I) (Fig. 3a: arrow). In sarcosyl-insoluble fraction, smear pattern was detected in TgαSYN#8812(T3), which accumulated much synuclein histologically. The anti-phosphorylated αSYN antibody pSyn#64 labeled the same size band as αSYN, 16 kD (Fig. 3b: arrow). These findings presented that sarcosyl-insoluble human αSYN and phosphorylated αSYN was accumulated in TgαSYN brains as reported in DLB brains (Hasegawa et al., 2002).

2.4. *Rotarod test for motor function of TgαSYN*

The rotarod test demonstrated that significant motor impairment appeared after a shorter time in TgαSYN; they dropped from the rotating rod faster than non-Tg littermates. The motor impairment was found at three months of age ($p<0.01$) and thereafter deteriorated with age ($p<0.001$. Fig. 4).

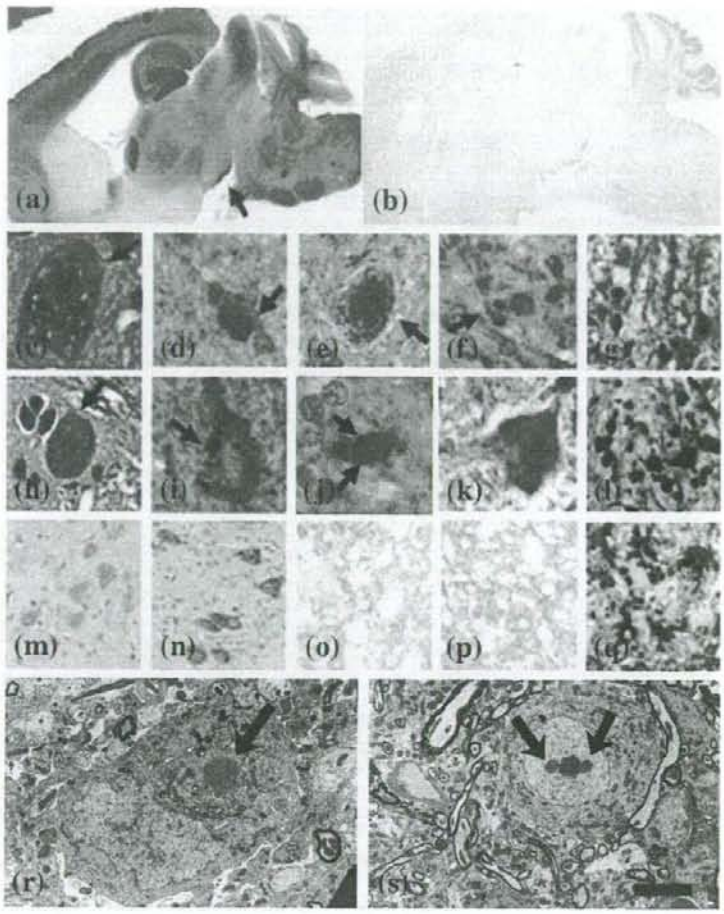

Fig. 2 – The pathological features of TgαSYN at seven months of age and age-matched non-Tg mice. (a) A sagittal section of a seven-month-old #8707 TgαSYN brain labeled by LB509 showed extensive αSYN accumulation prominently in the brainstem, hippocampus, thalamus, cerebellum and cerebral cortex. The substantia nigra of the midbrain is also labeled (arrow). The cerebral cortex and cerebellum showed atrophy. (b) No staining in the non-Tg mice brain by LB509. (c) Hematoxylin–eosin stain showed eosinophilic inclusion bodies and vacuoles in the cytoplasm of neurons in the substantia nigra of #8707 TgαSYN (arrow). (d) LB509 detected cytoplasmic inclusions in the substantia nigra of #8707 TgαSYN (arrow). (e) Anti-nitrated α/β SYN monoclonal antibody (Syn12) immunostained cytoplasmic inclusions in the substantia nigra (arrow), as well as in 14-month-old #8713 TgαSYN. (f) Ubiquitin-positive inclusions are shown in the substantia nigra of #8707 TgαSYN (arrow). (g) Ubiquitin-positive dystrophic neurites in the cerebellum dentate of 16-month-old #8713 TgαSYN. (h) Eosinophilic cytoplasmic inclusions (arrow) in the dentate nucleus of #8707 TgαSYN. (i) LB509-positive inclusion in the dentate nucleus of #8707 TgαSYN (arrow). (j) Cytoplasmic inclusions immunostained with a mouse monoclonal antibody 42/α-Synuclein in the brainstem of #8812 TgαSYN (arrow). (k) The PSer129 αSYN antibody immunostained the cytoplasm of neurons in the substantia nigra of #8707 TgαSYN. (l) Gallyas–Braak stain of dystrophic neurites in the dentate nucleus of a 16-month-old #8713 TgαSYN. (m) Tyrosine hydroxylase (TH) immuno-positive neurons in the locus ceruleus showed less immunostaining in the #8707 TgαSYN brain, than the non-Tg mouse brain (n). (o) The intensity of substance P immuno-positive synapses in the striatum of #8707 TgαSYN brain was lower than non-Tg mice brain (p). (q) Astrocytosis in the cerebellum of 16-month-old #8713 TgαSYN. (r) Electron-dense inclusions were found in the cytoplasm of neurons in the brainstems of 8-month-old #8718 TgαSYN by an EM study (arrow). (s) In the brainstem of the same mouse, intracellular inclusions (arrows) were also detected. Scale bar = 1 mm in a, b, 12.5 μm in c–f, h–k, 50 μm in g, l, m, n, 25 μm in o, p, and 0.38 μm in r, s.

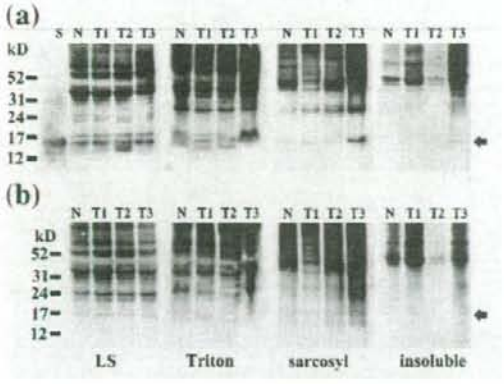

Fig. 3 – Western blot analysis. The expression of human αSYN was 16 kD (lane S; corresponded to recombinant human αSYN) by Western blot using antibody LB509 (a) and pSyn#64 (b) in LS-soluble (L), Triton-soluble (T), sarcosyl-soluble (S) and sarcosyl-insoluble (I) fractions of non-Tg (N), TgαSYN#8713 (T1), TgαSYN#8819 (T2), and TgαSYN#8812 (T3), 14-month-old mice brains.

2.5. *Measurement of neurochemicals*

There was no significant difference in brain weight among Tg and non-Tg mice at 10 and 17 months of age. Compared with age-matched non-Tg control mice, the levels of DA in the striatum were significantly decreased in 10 month-old ($p=0.0159$) and 17 month-old mice brains ($p=0.0286$). DA decreased approximately 17% to 24% in the striatum of TgαSYN brains (Fig. 5a). A significant decrease in DA was also detected in the hypothalamuses of 17-month-old TgαSYN brains ($p=0.0079$. Fig. 5b). NE was not decreased in any areas of 10-month-old TgαSYN brains (Fig. 5c). Serotonin was decreased in the hypothalamuses of 10- and 17-month-old TgαSYN brains ($p=0.0079$, $p=0.0286$, respectively. Fig. 5d). ACh decreased in the striatum in 17-month-old TgαSYN ($p=0.0286$. Fig. 5e). There was no significant alteration in DOPAC, HVA, MHPG, 5-HIAA and Ch levels in any areas of TgαSYN (data not shown). These results showed that insoluble mutant αSYN aggregation selectively decreased the DA level at 10 and 17 months of age.

3. Discussion

Several groups have already reported animal models of PD, such as wild-type αSYN Tg mice (Masliah et al., 2000), mutant αSYN Tg mice (van der Putten et al., 2000, Kahle et al., 2000, Giasson et al., 2002, Lee et al., 2002, Richfield et al., 2002, Neumann et al., 2002, Thiruchelvam et al., 2004, Tofaris et al. 2006, Wakamatsu et al., 2008), *Drosophila melanogaster* (Pendleton et al., 2002) and *C. elegans* (Kuwahara et al., 2006). The first αSYN Tg mice expressed wild-type human αSYN driven by the PDGF-β promoter (Masliah et al., 2000). This mouse displayed intraneuronal inclusions immunoreactive for αSYN and ubiquitin in several regions typically affected in α-synucleinopathies, while lacking the characteristic fibrillar components of Lewy bodies. The Tg mice overexpressing αSYN A53T developed under the murine Thy-1 regulatory sequence showed an early and dramatic decline in motor function (van der Putten et al., 2000). Transgenic wild-type and A30P αSYN abnormally accumulated in neuronal cell bodies and neurites throughout the brain (Kahle et al., 2000). Mice expressing wild-type or A53T αSYN under the mouse prion promoter developed motor deficits by eight months of age (Giasson et al., 2002). Neuropathological assessment of these Tg mice revealed a wide distribution of αSYN, with a pathological sparing of the motor cortex and a total sparing of the substantia nigra. Another group developed Tg mice harboring αSYN A53T using a mouse prion promoter showing motor dysfunction and αSYN accumulation (Lee et al., 2002). Truncated human αSYN (C-120) Tg mice under the TH promoter led to pathological changes in dopaminergic nerve cells of the substantia nigra and olfactory bulb (Tofaris et al., 2006). Recently, truncated human αSYN (C-130) Tg mice also led to selective loss of dopaminergic neurons and accumulation of phosphorylated αSYN (Wakamatsu et al., 2007, 2008).

One of the differences between these models and our TgαSYN was a novel combination of a promoter and mutation of αSYN. TgαSYN expressed double mutant αSYN with A30P +A53T under the human Thy-1 promoter. As expected, our TgαSYN demonstrated widespread αSYN accumulation in the brainstem, caudate putamen, cerebellum, hippocampus and cerebral cortex. Eosinophilic inclusion bodies in the substantia nigra and dentate nucleus of the cerebellum corresponded to accumulation of αSYN. Accumulated αSYN was ubiquitinated, nitrated and phosphorylated at the histological levels as shown in PD and DLB brain. Unfortunately, these inclusion bodies were not compatible with typical LBs because of the absence of a halo structure. At the EM level, fibrillar structure was not observed in inclusion bodies, but they were composed of massive aberrant fine granular structures. Aberrant inclusion bodies with modified αSYN were also observed widely. Since Gallyas–Braak staining labeled these LNs, accumulated αSYN in these neurites may have characteristics of those in β-sheet pleated structures.

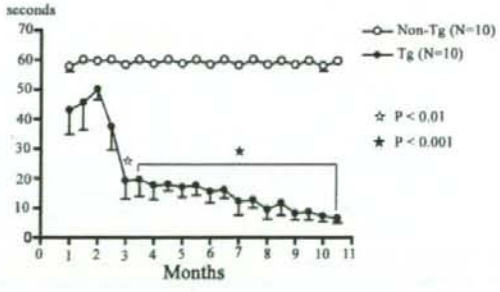

Fig. 4 – Rotarod test. The retention time of Tg mice on the rotarod significantly decreased in TgαSYN. The significant difference began to decrease at three months old (☆: $p<0.01$) and progressively deteriorated in an age-dependent manner from six months (★: $p<0.001$). Statistics were analyzed by two-way repeated measures ANOVA.

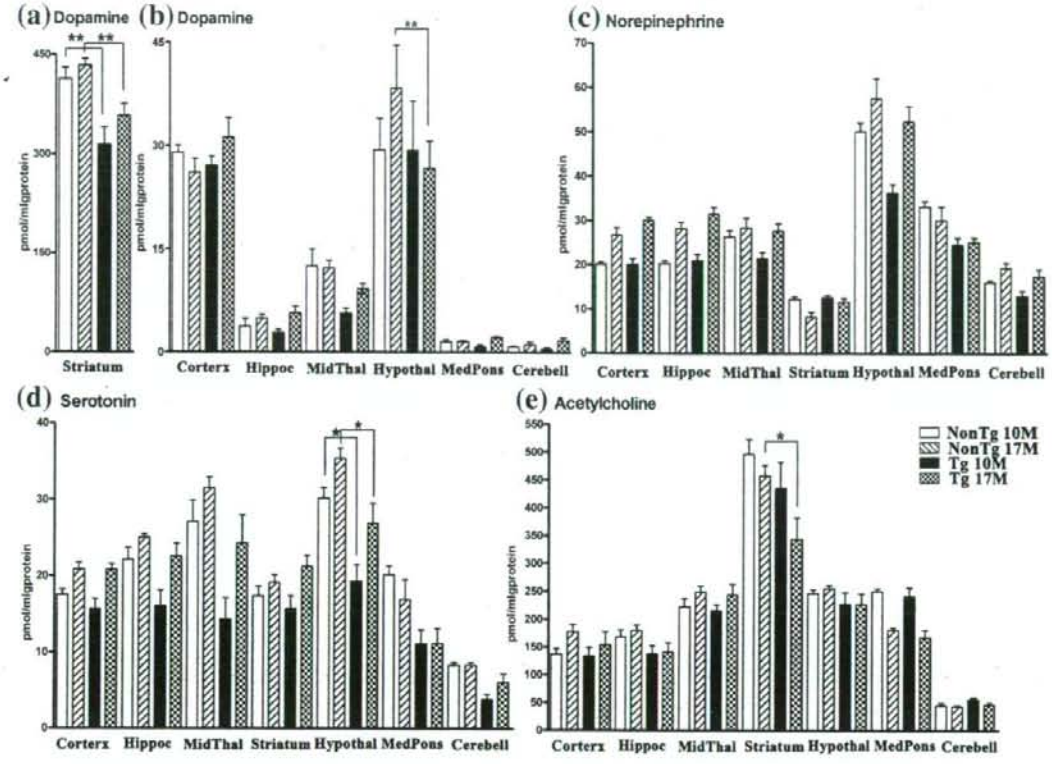

Fig. 5 – Measurement of neurochemicals. Opened column: 10-month-old non-Tg mice, Oblique column: 17-month-old non-Tg mice; Closed black colored column: 10-month-old TgαSYN mice, Crossed column: 17-month-old non-Tg mice. Cortex: cerebral cortex, Hippoc: hippocampus, MidThal: midbrain–thalamus, Hypothal: hypothalamus, MedPons: medulla–pons, Cerebell: cerebellum. *$p<0.01$, **$p<0.05$. Statistical analysis of neurochemicals between the TgαSYN and non-Tg control groups at the same age was conducted by a two-way repeated measure ANOVA (GraphPad Prism 4). (a) DA was significantly decreased in the striatum in 10- and 17-month-old TgαSYN compared with non-Tg control mice. (b) A decrease in dopamine was detected significantly in the hypothalamuses of 17-month-old TgαSYN brains ($p=0.0079$). (c) Norepinephrine (NE) was not decreased in 10- and 17-month-old TgαSYN brains. (d) Serotonin (5-HT) was decreased in the hypothalamus of 10- and 17-month-old TgαSYN brains ($p=0.0079$, $p=0.0286$, respectively). (e) ACh was decreased in the striatum of 17-month-old TgαSYN ($p=0.0286$).

The α-synuclein pathologies in TgαSYN were accompanied by decreased tyrosine hydroxylase-positive neurons, Substance P synapses and severe astrocytosis. These histological α-synuclein pathologies were also detected at the biochemical level. Accumulated αSYN was phosphorylated, ubiquitinated and sarcosyl-insoluble, suggesting that it may be conformationally changed as reported in PD/DLB brains (Hasegawa et al., 2002). The presence of higher molecule phosphorylated and ubiquitinated bands (22/29 kD) on Western blots also indicated that accumulated αSYN was modified and aggregated.

The severe decrease in DA and loss of dopaminergic neurons in SNc and the striata of PD brains is widely believed to be the pathological and biochemical cause of PD. Notably, our TgαSYN demonstrated decreased DA production in a disturbed DA system which was measured in the liquid chromatographic systems. Although other neurochemicals were altered slightly, a prominently decreased level of DA was revealed in the striatum of TgαSYN. These findings suggest selective neurotoxicity with αSYN accumulation.

In our mouse model, approximately a 20% reduction in DA in the striatum was observed when motor impairment existed. Since the rotarod test revealed significant decreased spontaneous movement, the phenotype of TgαSYN is quite similar to the cardinal clinical symptom of PD, akinesia. A decreased level of TH-positive neurons and substance P synapses also suggested that the motor impairment in TgαSYN may be caused by aberrant αSYN processes.

Our TgαSYN is a mammalian model animal showing decreased DA and motor deficits, which were certainly detected by the liquid chromatographic systems and rotarod test. For this reason, TgαSYN is a useful model for analyzing the aberrant cascade induced by pathological metabolism and aggregation of mutant αSYN, and may be useful for developing essential treatments for α-synucleinopathies such as PD and DLB.

4. Experimental procedures

4.1. *Transgene construction, generation of transgenic mice and analyses of RT-PCR*

Human αSYN A30P+A53T cDNA (450 bp) was ligated into Hind III sites in the human Thy-1 genome gene. The transgene hThy1-αSYN A30P+A53T consisted of an 8.1 kb XhoI–NcoI fragment of pBluescript II KS kidney enhancer (Fig. 1a). The CX-EGFP transgene consisted of a 3 kb Xba I/BamH I fragment of pCAGGS containing the CMV enhancer, β-actin promoter, a part of the rabbit β-globin gene, a part of the second intron, the third exon and 3′-untranslated region and cDNA of EGFP (Enhanced green fluorescent protein) with the Kozak sequence (Imai et al., 1999). Approximately 2,000 copies of the transgene with a 1:1 mole rate mixture of the hThy1-αSYN A30P+A53T and CX-EGFP as a transgene marker were micro-injected into the pronuclei of fertilized BDF1 eggs. To analyze gene expression of human αSYN, RT-PCR was performed using 2 μl of mRNA, isolated using the QuickPrep Micro mRNA purification kit (GE Healthcare Bio-Sciences Corp., Piscataway, NJ), from the brains of TgαSYN (#8713) and non-Tg mice brains at 3, 8, 17 months of age ($n=3$, respectively) in the reaction tube of Ready-To-Go RT-PCR Beads (GE Healthcare Bio-Sciences Corp., Piscataway, NJ) with PCR primer sets as follows: (αSYN forward primer: TG GAT GTA TTC ATG AAA GGA, αSYN reverse primer: CC AGT GGC TGC TGC AAT GCT C; EGFP forward primer: TGG TGA GCA AGG GCG AGG AG; EGFP reverse primer: TCG TGC TGC TTC ATG TGG TC). For semi-quantification, RT-PCR of β-actin was performed as an internal control (Elliott, 2001). Ten microliters of PCR products were analyzed by 2.5% agarose gel electrophoresis. The intensity of ethidium-stained bands was analyzed by Scion Image (Scion Corporation, Frederick, MD).

4.2. *Histological examinations*

After mice were sacrificed under anesthesia, the brains were removed and cut sagittally along the midline. One hemisphere was fixed in 0.1 mol/L phosphate buffer (PB, pH 7.6) containing 4% paraformaldehyde, and embedded in paraffin. For immunostaining, 5-μm sections were treated with 99% formic acid for 3 min, or treated in a microwave at 500 W for 5 min three times in 10 mmol/L citrate buffer (pH 6.0). After blocking with 5% normal goat or horse serum in 50 mmol/L phosphate buffered saline (PBS) containing 0.05% Tween-20 and 4% Block-Ace (Snow brand, Sapporo, Japan), sections were incubated with primary antibodies for 6 h. Specific labeling was visualized using a Vectastain Elite ABC kit (Vector, Burlingame, CA). Immunostained tissue sections were counterstained with hematoxylin. Nissl, Hematoxylin–eosin (H–E), and Gallyas–Braak stains were also done.

The following antibodies were used: mouse monoclonal antibody to human αSYN, LB509 (×4, residues 115–121/122) (Baba et al., 1998); mouse monoclonal antibody to αSYN, 42/α-Synuclein (×50, BD Transduction Laboratories, San Jose, CA); rabbit polyclonal antibody to phosphorylated Serine at residue 129 of human αSYN, PSer129 (×200) (Fujiwara et al., 2002; Hasegawa et al., 2002); rabbit polyclonal antibody to tyrosine hydroxylase (TH), AB151 (×2,000, CHEMICON, Temecula, CA); rabbit polyclonal antibody to substance P, AB1566 (×1,000, CHEMICON, Temecula, CA); rabbit polyclonal antibody to ubiquitin, UbiQ (×500) (Ikeda et al., 2005; Murakami et al., 2006); mouse monoclonal antibody to nitrated α/β SYN, Syn12 (×400, Invitrogen, Corps., Carlsbad, CA); rabbit polyclonal antibody to glial fibrillary acidic protein (GFAP, ×20,000, DAKO, Carpinteria, CA).

For electron microscopic (EM) studies, the brain tissues were immersed in a fixative solution (2.5% glutaraldehyde, 0.1 mol/L phosphate buffer (PB), pH 7.4) for 4 h and washed several times in 0.1 mol/L PB containing 7% sucrose. Blocks were then postfixed in 2% osmium tetroxide, dehydrated in ethanol and propylene oxide, and embedded in Quetol 812 (Nisshin EM, Tokyo, Japan). Ultrathin sections were stained with uranyl acetate and lead acetate prior to observation.

4.3. *Western blot analysis*

Half of each brain was homogenized in 3 ml/g of low-salt buffer (LS: 10 mmol/L Tris, 5 mmol/L ethylenediaminetetraacetic acid (EDTA), 1 mmol/L dithiothreitol (DTT), 10% sucrose, and a cocktail of protease inhibitors (Complete®, Roche Diagnostics, Indianapolis, IN), pH 7.5) and centrifuged at 25,000 g for 30 min at 4 °C (LS-soluble fraction). Pellets were treated with 3 ml/g of LS with 1% Triton X-100 and 0.5 mol/L NaCl, and centrifuged at 180,000 g for 30 min at 4 °C (Triton-soluble fraction). Pellets were then homogenized again in 2 ml/g LS with 1% N-lauroylsarcosine (SIGMA CHEMICAL CO. St Louis, MO) and 0.5 mol/L NaCl, incubated at 22 °C on a shaker for 1 h, and centrifuged at 180,000 g for 30 min at 22 °C. Supernatants were analyzed as sarcosyl-soluble fraction (Iwatsubo et al., 1996; Hasegawa et al., 2002; Sampathu et al., 2003; Ikeda et al., 2005; Murakami et al., 2006). The remaining pellets obtained from each sarcosyl-insoluble fraction were boiled at 70 °C in 20 μl of NuPAGE® LDS Sample Buffer for 10 min. Each fraction was separated on 4 to 12% NuPAGE Bis–Tris Gels (Invitrogen, Corps., Carlsbad, CA) and the blots were labeled by a mouse monoclonal antibody to human αSYN (LB509, ×4), and a mouse monoclonal antibody to phosphorylated Serine at residue 129 of human αSYN (pSyn#64, ×200, Wako, Japan). Signals were visualized with an enhanced chemiluminescence detection system (SuperSignal West® Dura Extended Duration Substrate, PIERCE, Rockford, IL) and quantified by a luminoimage analyzer (LAS 1000-mini, Fuji film, Tokyo, Japan).

4.4. *Measurement of neurochemicals*

Neurochemicals, including dopaminergic (dopamine: DA, 3,4-dihydroxyphenylacetic acid: DOPAC, homovanillic acid: HVA), noradrenergic (norepinephrine: NE, 3-methoxy-4hydroxyphenylglycol: MHPG), serotonergic (5-hydroxytryptamine: 5-HT, 5-hydroxyindoleacetic acid: 5-HIAA) and cholinergic (acetylcholine: ACh, choline: Ch) systems in the brain were measured in Tg mice ($n=10$) and non-Tg control mice ($n=10$) at 10 and 17 months old, respectively. In brief, each animal was anesthetized with Nembutal® (Dainippon Pharmaceutical Co. Ltd., pentobarbital sodium), sacrificed, and irradiated with microwaves (NJE 2603 Microwave device, New Japan Radio, Kamifukuoka, Japan) at 9.0 kW for 0.42 s to prevent post-mortem

changes in the neurochemicals during brain sampling (Ikarashi et al., 1985, 2004). The brain was removed from the skull and dissected into seven regions (cerebral cortex, hippocampus, midbrain–thalamus, striatum, hypothalamus, medulla–pons and cerebellum) according to the established method (Glowinski and Iversen, 1966), and then each region was weighed. Each dissected brain region was homogenized with 0.5 ml of 0.1 mol/L perchloric acid containing 0.8 nmol isoproterenol hydrochloride as an internal standard for the determinations of catecholamines, indoleamines and related metabolites, and 5 nmol ethylhomocholine iodide as an internal standard for the determinations of ACh and Ch, using an ultrasonic cell disrupter (US-300T, Nissei, Tokyo, Japan). The homogenate was centrifuged at 17,300 g at 4 °C for 15 min. The supernatant was filtered through a 0.45 μm millipore filter. Aliquots, typically 10 μl of the filtrates, were injected into the liquid chromatographic systems (Eicom HPLC-ECD system, Eicom Co. Ltd., Kyoto, Japan) to determine catecholamines-, indoleamines-, and acetylcholine-related substances (Ikarashi et al., 1992). The sediment was re-homogenized with 2 ml of 1 mol/L NaOH for a protein assay, which was performed using the method of Lowry et al. (1951). The concentrations of neurochemicals in the brain were expressed as the values per milligram of protein.

4.5. *Behavioral experiments*

4.5.1. *Rotarod test*

TgαSYN ($n=10$) and age-matched control mice ($n=10$) at one month to 10.5 months old were examined by the rotarod performance test according to a previous method (Kuribara et al., 1977; Ikarashi et al., 2004). Mice were placed on the rotating rod of the apparatus (Ugo basile, biological research apparatus, Milan, Italy) at a speed of 16 rpm for 300 s, and the time they stayed on the rotating rod was measured. Each set of three trials was performed at 10 minute intervals each day for every mouse.

4.6. *Statistical analyses*

Two-way repeated measures ANOVA followed by the Mann–Whitney U test for the rotarod test and open field test, and two-way ANOVA followed by Student's t test to analyze neurochemicals were performed using GraphPad Prism 4 (GraphPad Software Inc., San Diego, CA) and SPSS 10.0 (SPSS 10.0 for Windows, SPSS Inc., Chicago, IL). The means of all data are presented with their standard errors (mean±S.E.).

Acknowledgments

We thank Dr. T Iwatsubo for coordinative provision of the LB 509 antibody and polyclonal phosphorylated αSYN antibody, Dr. D Dickson for the antibody Ubi-Q and Dr. S Kawabata for the human Thy-1 gene. We thank Dr. H Sugimoto and Dr. T Izumi for technical supports, and Dr. J Hirato for kind coordinative support. We also thank Y Nogami and H Narihiro for technical assistance. All animal experiments were performed according to guidelines established in the "Guide for the Care and Use of Laboratory Animals" (Japan).

REFERENCES

Abeliovich, A., Schmitz, Y., Farinas, I., Choi-Lundberg, D., Ho, W.H., Castillo, P.E., Shinsky, N., Verdugo, J.M., Armanini, M., Ryan, A., Hynes, M., Phillips, H., Sulzer, D., Rosenthal, A., 2000. Mice lacking α-synuclein display functional deficits in the nigrostriatal-DOPAmine system. Neuron 25, 239–252.

Arai, K., Kato, N., Kashiwado, K., Hattori, T., 2000. Pure autonomic failure in association with human α-synucleinopathy. Neurosci. Lett. 296, 171–173.

Baba, M., Nakajo, S., Tu, P.H., Tomita, T., Nakaya, K., Lee, V.M., Trojanowski, J.Q., Iwatsubo, T., 1998. Aggregation of α-synuclein in Lewy bodies of sporadic Parkinson's disease and dementia with Lewy bodies. Am. J. Pathol. 152, 879–884.

Chartier-Harlin, M.C., Kachergus, J., Roumier, C., Mouroux, V., Douay, X., Lincoln, S., Levecque, C., Larvor, L., Andrieux, J., Hulihan, M., Waucquier, N., Defebvre, L., Amouyel, P., Farrer, M., Destée, A., 2004. -Synuclein locus duplication as a cause of familial Parkinson's disease. Lancet 364, 1167–1169.

Chen, X., de Silva, H.A., Pettenati, M.J., Rao, P.N., St. George-Hyslop, P., Roses, A.D., Xia, Y., Horsburgh, K., Ueda, K., Saitoh, T., 1995. The human NACP/α-synuclein gene: chromosome assignment to 4q21.3–q22 and TaqI RFLP analysis. Genomics 26, 425–427.

Chishti, M.A., Yang, D.S., Janus, C., Phinney, A.L., Horne, P., Pearson, J., Strome, R., Zuker, N., Loukides, J., French, J., Turner, S., Lozza, G., Grilli, M., Kunicki, S., Morissette, C., Paquette, J., Gervais, F., Bergeron, C., Fraser, P.E., Carlson, G.A., George-Hyslop, P.S., Westaway, D., 2001. Early-onset amyloid deposition and cognitive deficits in transgenic mice expressing a double mutant form of amyloid precursor protein 695. J. Biol. Chem. 276, 21562–21570.

Choi, W., Zibaee, S., Goedert, M., 2004. Mutation increases phospholipids binding and assembly into filaments of human α-synuclein. FEBS Lett. 576, 363–368.

Citron, M., Eckman, C.B., Diehl, T.S., Corcoran, C., Ostaszewski, B. L., Xia, W., Levesque, G., St. George-Hyslop, P., Younkin, S.G., Selkoe, D.J., 1998. Additive effects of PS1 and APP mutations on secretion of the 42-residue amyloid β-protein. Neurobiol. Dis. 5, 107–116.

Clayton, D.F., George, J.M., 1998. The synucleins: a family of proteins involved in synaptic function, plasticity, neurodegeneration and disease. Trends. Neurosci. 21, 249–254.

Conway, K.A., Rochet, J.C., Bieganski, R.M., Lansbury Jr., P.T., 2001. Kinetic stabilization of the α-synuclein protofibril by a dopamine-α-synuclein adduct. Science 294, 1346–1349.

Elliott, J.L., 2001. Cytokine upregulation in a murine model of familial amyotrophic lateral sclerosis. Brain Res. Mol. Brain Res. 95, 172–178.

Fujiwara, H., Hasegawa, M., Dohmae, N., Kawashima, A., Masliah, E., Goldberg, M.S., Shen, J., Takio, K., Iwatsubo, T., 2002. -Synuclein is phosphorylated in synucleinopathy lesions. Nat. Cell Biol. 4, 160–164.

Galvin, J.E., Giasson, B., Hurtig, H.I., Lee, V.M., Trojanowski, J.Q., 2000. Neurodegeneration with brain iron accumulation, type 1 is characterized by α-, β-, and γ-synuclein neuropathology. Am. J. Pathol. 157, 361–368.

George, J.M., Jin, H., Woods, W.S., Clayton, D.F., 1995. Characterization of a novel protein regulated during the critical period for song learning in the zebra finch. Neuron 15, 361–372.

Giasson, B.I., Duda, J.E., Quinn, S.M., Zhang, B., Trojanowski, J.Q., Lee, V.M., 2002. Neuronal α-Synucleinopathy with severe movement disorder in mice expressing A53T human α-synuclein. Neuron 34, 521–533.

Glowinski, J., Iversen, L.L., 1966. Regional studies of catecholamines in the rat brain. I. The disposition of [^{3}H]norepinephrine, [^{3}H]dopamine and [^{3}H]dopa in various regions of the brain. J. Neurochem. 13, 655–669.

Goedert, M., 2000. -synuclein and neurodegenerative diseases. Nat. Rev. Neurosci. 2, 492–501.
Hardy, J., Gwinn-Hardy, K., 1998. Genetic classification of primary neurodegenerative disease. Science 282, 1075–1079.
Hasegawa, M., Fujiwara, H., Nonaka, T., Wakabayashi, K., Takahashi, H., Lee, V.M., Trojanowski, J.Q., Mann, D., Iwatsubo, T., 2002. Phosphorylated α-synuclein is ubiquitinated in alpha-synucleinopathy lesions. J. Biol. Chem. 277, 49071–49076.
Ikarashi, Y., Harigaya, Y., Tomidokoro, Y., Kanai, M., Ikeda, M., Matsubara, E., Kawarabayashi, T., Kuribara, H., Younkin, S.G., Maruyama, Y., Shoji, M., 2004. Decreased level of brain acetylcholine and memory disturbance in APPsw mice. Neurobiol. Aging 25, 483–490.
Ikarashi, Y., Sasahara, T., Maruyama, Y., 1985. Postmortem changes in catecholamines, indoleamines, and their metabolites in rat brain regions: prevention with 10-kW microwave irradiation. J. Neurochem. 45, 935–939.
Ikarashi, Y., Blank, C.L., Maruyama, Y., 1992. Glassy carbon pre-column for determination of acetylcholine and choline in biological samples using liquid chromatography with electrochemical detection. J. Chromatogr. 575, 29–37.
Ikeda, M., Shoji, M., Kawarai, T., Kawarabayashi, T., Matsubara, E., Murakami, T., Sasaki, A., Tomidokoro, Y., Ikarashi, Y., Kuribara, H., Ishiguro, K., Hasegawa, M., Yen, S.H., Chishti, M.A., Harigaya, Y., Abe, K., Okamoto, K., St George-Hyslop, P., Westaway, D., 2005. Accumulation of filamentous tau in the cerebral cortex of human tau R406W transgenic mice. Am. J. Pathol. 166, 521–531.
Imai, E., Akagi, Y., Isaka, Y., Ikawa, M., Takenaka, M., Hori, M., Okabe, M., 1999. Glowing podocytes in living mouse: transgenic mouse carrying a podocyte-specific promoter. Exp. Nephrol. 7, 63–66.
Iwai, A., Masliah, E., Yoshimoto, M., Ge, N., Flanagan, L., de Silva, H. A., Kittel, A., Saitoh, T., 1995. The precursor protein of non-Aβ component of Alzheimer's disease amyloid is a presynaptic protein of the central nervous system. Neuron 14, 467–475.
Iwatsubo, T., Yamaguchi, H., Fujimuro, M., Yokosawa, H., Ihara, Y., Trojanowski, J.Q., Lee, V.M., 1996. Purification and characterization of Lewy bodies from the brains of patients with diffuse Lewy body disease. Am. J. Pathol. 148, 1517–1529.
Kahle, P.J., Neumann, M., Ozmen, L., Muller, V., Jacobsen, H., Schindzielorz, A., Okochi, M., Leimer, U., van der Putten, H., Probst, A., Kremmer, E., Kretzschmar, H.A., Haass, C., 2000. Subcellular localization of wild-type and Parkinson's disease-associated mutant α-synuclein in human and transgenic mouse brain. J. Neurosci. 20, 6365–6373.
Kitada, T., Asakawa, S., Hattori, N., Matsumine, H., Yamamura, Y., Minoshima, S., Yokochi, M., Mizuno, Y., Shimizu, N., 1998. Mutations in the parkin gene cause autosomal recessive juvenile parkinsonism. Nature 392, 605–608.
Kruger, R., Kuhn, W., Muller, T., Woitalla, D., Graeber, M., Kosel, S., Przuntek, H., Epplen, J.T., Schols, L., Riess, O., 1998. Ala30Pro mutation in the gene encoding α-synuclein in Parkinson's disease. Nat. Genet. 18, 106–108.
Kuribara, H., Higuchi, Y., Tadokoro, S., 1977. Effects of central depressants on rota-rod and traction performances in mice. Jpn. J. Pharmacol. 27, 117–126.
Lee, M.K., Stirling, W., Xu, Y., Xu, X., Qui, D., Mandir, A.S., Dawson, T.M., Copeland, N.G., Jenkins, N.A., Price, D.L., 2002. Human α-synuclein-harboring familial Parkinson's disease-linked Ala-53. Thr mutation causes neurodegenerative disease with α-synuclein aggregation in transgenic mice. Proc. Natl. Acad. Sci. U. S. A. 99, 8968–8973.
Liscovitch, M., Czarny, M., Fiucci, G., Tang, X., 2000. Phospholipase D: molecular and cell biology of a novel gene family. Biochem. J. 345, 401–415.
Lotharius, J., Brundin, P., 2000. Pathogenesis of Parkinson's disease: dopamine, vesicles and α-synuclein. Nat. Rev. Neurosci. 3, 932–942.
Lowry, O.H., Rosebrough, N.J., Farr, A.L., Randall, R.J., 1951. Protein measurement with the Folin phenol reagent. J. Biol. Chem. 193, 265–275.
Masliah, E., Rockenstein, E., Veinbergs, I., Mallory, M., Hashimoto, M., Takeda, A., Sagara, Y., Sisk, A., Mucke, L., 2000. L-DOPAminergic loss and inclusion body formation in α-synuclein mice: implications for neurodegenerative disorders. Science 287, 1265–1269.
Murakami, T., Paitel, E., Kawarabayashi, T., Ikedame>M., Chishti, M.A., Janus, C., Matsubara, E., Sasaki, A., Kawarai, T., Phinney, A.L., Harigaya, Y., Horne, P., Egashira, N., Mishima, K., Hanna, A., Yang, J., Iwasaki, K., Takahashi, M., Fujiwara, M., Ishiguro, K., Bergeron, C., Carlson, G.A., Abe, K., Westaway, D., St. George-Hyslop, P., Shoji, M., 2006. Cortical neuronal and glial pathology in TgTauP301L transgenic mice: neuronal degeneration, memory disturbance, and phenotypic variation. Am. J. Pathol. 169, 1343–1352.
Neumann, M., Kahle, P.J., Giasson, B.I., Ozmen, L., Borroni, E., Spooren, W., Muller, V., Odoy, S., Fujiwara, H., Hasegawa, M., 2002. Misfolded proteinase K-resistant hyperphosphorylated α-synuclein in aged transgenic mice with locomotor deterioration and in human α-synucleinopathies. J. Clin. Invest. 110, 1429–1439.
Payton, J.E., Perrin, R.J., Woods, W.S., George, J.M., 2000. Structural determinants of PLD2 inhibition by α-synuclein. J. Mol. Biol. 337, 1001–1009.
Polymeropoulos, M.H., Lavedan, C., Leroy, E., Ide, S.E., Dehejia, A., Dutra, A., Pike, B., Root, H., Rubenstein, J., Boyer, R., Stenroos, E.S., Chandrasekharappa, S., Athanassiadou, A., Papapetropoulos, T., Johnson, W.G., Lazzarini, A.M., Duvoisin, R.C., Di Iorio, G., Golbe, L.I., Nussbaum, R.L., 1997. Mutation in the α-synuclein gene identified in families with Parkinson's disease. Science 276, 2045–2047.
Richfield, E.K., Thiruchelvam, M.J., Cory-Slechta, D.A., Wuertzer, C., Gainetdinov, R.R., Caron, M.G., Di Monte, D.A., Federoff, H.J., 2002. Behavioral and neurochemical effects of wild-type and mutated human alpha-synuclein in transgenic mice. Exp. Neurol. 175, 35–48.
Sampathu, D.M., Giasson, B.I., Pawlyk, A.C., Trojanowski, J.Q., Lee, V.M., 2003. Ubiquitination of α-synuclein is not required for formation of pathological inclusions in α-synucleinopathies. Am. J. Pathol. 163, 91–100.
Shimura, H., Schlossmacher, M.G., Hattori, N., Frosch, M.P., Trockenbacher, A., Schneider, R., Mizuno, Y., Kosik, K.S., Selkoe, D.J., 2001. Ubiquitination of a new form of α-synuclein by parkin from human brain: implications for Parkinson's disease. Science 293, 263–269.
Shoji, M., Harigaya, Y., Sasaki, A., Ueda, K., Ishiguro, K., Matsubara, E., Watanabe, M., Ikeda, M., Kanai, M., Tomidokoro, Y., Shizuka, M., Amari, M., Kosaka, K., Nakazato, Y., Okamoto, K., Hirai, S., 2000. Accumulation of NACP/α-synuclein in Lewy body disease and multiple system atrophy. J. Neurol. Neurosurg. Psychiatry 68, 605–608.
Singleton, A.B., Farrer, M., Johnson, J., Singleton, A., Hague, S., Kachergus, J., Hulihan, M., Peuralinna, T., Dutra, A., Nussbaum, R., Lincoln, S., Crawley, A., Hanson, M., Maraganore, D., Adler, C., Cookson, M.R., Muenter, M., Baptista, M., Miller, D., Blancato, J., Hardy, J., Gwinn-Hardy, K., 2002. -Synuclein locus triplication causes Parkinson's disease. Science 302, 841.
Spillantini, M.G., Schmidt, M.L., Lee, V.M., Trojanowski, J.Q., Jakes, R., Goedert, M., 1997. -synuclein in Lewy bodies. Nature 388, 839–840.
Thiruchelvam, M.J., Powers, J.M., Cory-Slechta, D.A., Richfield, E.K., 2004. Risk factors for dopaminergic neuron loss in human α-synuclein transgenic mice. Eur. J. Neurosci. 19, 845–854.
Tofaris, G.K., Reitböck, P.G., Humby, T., Lambourne, S.L., O'Connell, M., Ghetti, B., Gossage, H., Emson, P.C., Wilkinson, L.S., Goedert, M., Spillantini, M.G., 2006. Pathological changes in dopaminergic nerve cells of the substantia nigra and olfactory bulb in mice transgenic for truncated human

α-synuclein(1–120): implications for Lewy body disorders. J. Neurosci. 26, 3942–3950.

Tu, P.H., Galvin, J.E., Baba, M., Giasson, B., Tomita, T., Leight, S., Nakajo, S., Iwatsubo, T., Trojanowski, J.Q., Lee, V.M., 1998. Glial cytoplasmic inclusions in white matter oligodendrocytes of multiple system atrophy brains contain insoluble α-synuclein. Ann. Neurol. 44, 415–422.

Ueda, K., Fukushima, H., Masliah, E., Xia, Y., Iwai, A., Yoshimoto, M., Otero, D.A., Kondo, J., Ihara, Y., Saitoh, T., 1992. Molecular cloning of cDNA encoding an unrecognized component of amyloid in Alzheimer disease. Proc. Natl. Acad. Sci. U. S. A. 90, 11282–11286.

van der Putten, H., Wiederhold, K.H., Probst, A., Barbieri, S., Mistl, C., Danner, S., Kauffmann, S., Hofele, K., Spooren, W.P., Ruegg, M.A., Lin, S., Caroni, P., Sommer, B., Tolnay, M., Bilbe, G., 2000. Neuropathology in mice expressing human α-synuclein. J. Neurosci. 20, 6021–6029.

Wakamatsu, M., Ishii, A., Ukai, Y., Sakagami, J., Iwata, S., Ono, M., Matsumoto, K., Nakamura, A., Tada, N., Kobayashi, K., Iwatsubo, T., Yoshimoto, M., 2007. Accumulation of phosphorylated α-synuclein in dopaminergic neurons of transgenic mice that express human α-synuclein J. Neurosci. Res. 85, 1819–1825.

Wakamatsu, M., Ishii, A., Iwata, S., Sakagami, J., Ukai, Y., Ono, M., Kanbe, D., Muramatsu, S., Kobayashi, K., Iwatsubo, T., Yoshimoto, M., 2008. Selective loss of nigral dopamine neurons induced by overexpression of truncated human α-synuclein in mice. Neurobiol. Aging 29, 574–585.

Zarranz, J.J., Alegre, J., Gomez-Esteban, J.C., Lezcano, E., Ros, R., Ampuero, I., Vidal, L., Hoenicka, J., Rodriguez, O., Atares, B., Llorens, V., Gomez Tortosa, E., del Ser, T., Munoz, D.G., de Yebenes, J.G., 2004. The new mutation, E46K, of α-synuclein causes Parkinson and Lewy body dementia. Ann. Neurol. 55, 164–173.

BRAIN RESEARCH 1219 (2008) 169–179

available at www.sciencedirect.com

ScienceDirect

www.elsevier.com/locate/brainres

BRAIN RESEARCH

Research Report

Plasma antibodies to Aβ40 and Aβ42 in patients with Alzheimer's disease and normal controls

Wuhua Xu[a,b], Takeshi Kawarabayashi[c], Etsuro Matsubara[d], Kentaro Deguchi[a], Tetsuro Murakami[a], Yasuo Harigaya[e], Masaki Ikeda[f], Masakuni Amari[g], Ryozo Kuwano[h], Koji Abe[a], Mikio Shoji[c,]*

[a]*Department of Neurology, Neuroscience, Biophysiological Science, Okayama University Graduate School of Medicine, Dentistry and Pharmacy, 2-5-1 Shikatacho, Okayama 700-8558, Japan*
[b]*Department of Neurology, Guangzhou Red Cross Hospital, Fourth Affiliated Hospital of Jinan University Medical College, Guangzhou 510220, China*
[c]*Department of Neurology, Hirosaki University Graduate School of Medicine, 5 Zaifu-cho, Hirosaki, Aomori 036-8562, Japan*
[d]*Department of Alzheimer's Disease Research, National Institute for Longevity Sciences, 36-3 Gengo, Morioka, Obu, Aichi 474-8522, Japan*
[e]*Department of Neurology, Maebashi Red Cross Hospital, 3-21-36, Asahimachi, Maebashi, Gunma 371-0014, Japan*
[f]*Department of Neurology, Gunma University School of Medicine, 3-39-22 Showamachi, Maebashi, Gunma 371-8511, Japan*
[g]*Department of Neurology, Geriatrics Research Hospital, 3-26-8 Otomomachi, Maebashi, Gunma 371-0847, Japan*
[h]*Department of Bioinformatics, Genome Science Branch, Center for Bioresource-based Researches, Brain Research Institute, Niigata University, 1-757 Asahimachi, Niigata 951-8122, Japan*

ARTICLE INFO

Article history:
Accepted 15 February 2008
Available online 4 March 2008

Keywords:
Amyloid
Aβ
Alzheimer's disease
Antibodies
Plasma

ABSTRACT

Antibodies to amyloid β protein (Aβ) are present naturally or after Aβ vaccine therapy in human plasma. To clarify their clinical role, we examined plasma samples from 113 patients with Alzheimer's disease (AD) and 205 normal controls using the tissue amyloid plaque immunoreactivity (TAPIR) assay. A high positive rate of TAPIR was revealed in AD (45.1%) and age-matched controls (41.2%), however, no significance was observed. No significant difference was observed in the MMS score or disease duration between TAPIR-positive and negative samples. TAPIR-positive plasma reacted with the Aβ40 monomer and dimer, and the Aβ42 monomer weakly, but not with the Aβ42 dimer. TAPIR was even detected in samples from young normal subjects and young Tg2576 transgenic mice. Although the Aβ40 level and Aβ40/42 ratio increased, and Aβ42 was significantly decreased in plasma from AD groups when compared to controls, no significant correlations were revealed between plasma Aβ levels and TAPIR grading. Thus an immune response to Aβ40 and immune tolerance to Aβ42 occurred naturally in humans without a close relationship to the Aβ burden in the brain. Clarification of the mechanism of the immune response to Aβ42 is necessary for realization of an immunotherapy for AD.

1. Introduction

AD brains are invariably characterized by two pathological features: initial Aβ amyloidosis characterized by extracellular deposition of Aβ42 (43) and Aβ40, and subsequent tauopathy characterized by intracellular accumulation of neurofibrillary tangles consisting of abnormally phosphorylated tau. Since familial AD-linked mutations of amyloid β protein precursor

* *Corresponding author.* Fax: +81 172 39 5143.
E-mail address: mshoji@cc.hirosaki-u.ac.jp (M. Shoji).

0006-8993/$ – see front matter © 2008 Elseveir B.V. All rights reserved.
doi:10.1016/j.brainres.2008.02.060

(βAPP), presenilin-1 (PS-1), and presenilin-2 (PS-2) increase the extracellular concentration of Aβ42 (43) and protofibril Aβ, these peptides are likely to be initiating factors in the pathogenesis of all types of AD (Hardy and Selkoe, 2002, Selkoe, 2002). Transgenic mouse models reproducing substantial brain Aβ amyloid support these hypotheses, and the appearance of neurofibrillary tangles (NFT) enhanced by Aβ amyloid in Tg2576 x tau P301L double transgenic mice further indicates that Aβ amyloidosis is the most important target for curing AD (Lewis et al., 2001).

Recent studies suggested that Aβ immunotherapy is the most promising among the many candidate therapies for AD. Schenk and others showed that an Aβ42 peptide vaccine clearly reduced the Aβ amyloid burden in transgenic model mice (Schenk et al., 1999; Weiner et al., 2000; Janus et al., 2000; Morgan et al., 2000). Passive immunization using anti-Aβ antibodies was also shown to be effective for reduction of the Aβ amyloid burden (Bard et al., 2000). These findings suggest peripheral antibodies to Aβ may serve a protective role against AD. A detectable increase in antibodies to Aβ42 was observed in about 25% of patients who received AN1792 in a Phase I study (Orgogozo et al., 2003; Nicoll et al., 2003). Analysis of serum samples by ELISA indicated that 15 of 18 patients experiencing meningoencephalitis in a Phase II study had antibodies against Aβ42. CSF antibodies to Aβ42 were present in 6 of 8 patients tested after the onset of encephalitis. However, titers of antibodies to Aβ42 were not correlated with the occurrence or severity of symptoms or relapses (Orgogozo et al., 2003). An autoantibody to Aβ40 was first detected in human B cell lines from AD patients (Gaskin et al., 1993). Naturally occurring antibodies to synthetic Aβ40 were confirmed by ELISA in the CSF and plasma of non-immunized humans and titers were significantly higher in healthy controls than in patients with AD (Du et al., 2001). Titers of anti-Aβ42 peptide antibodies were lower in AD patients compared with healthy individuals (Weksler et al., 2002), or elevated in AD patients and elder transgenic mice (Nath et al., 2003). Naturally occurring anti-Aβ42 antibodies were detected at very low levels by ELISA in over 50% of elderly individuals and at modest levels in 5% of them. Neither the presence nor the amount of naturally occurring anti-Aβ42 antibodies correlated with the presence, or age of AD onset, or the plasma levels of Aβ40 and Aβ42 (Hyman et al., 2001). Normal levels of antibodies to Aβ42 and Aβ40 were present in both AD and control groups, even in a young population (Baril et al., 2004). Thus, the previous reports suggested complex relationships for naturally occurring antibodies to Aβ.

In the Zurich cohort of a Phase II study, patients who generated antibodies to β-amyloid plaques in the plasma as determined by tissue amyloid plaque immunoreactivity (TAPIR) assay showed significantly slower rates of decline for cognitive functions and daily living activities suggesting that antibodies against β-amyloid plaques may be protective against AD (Hock et al., 2002, 2003; Gilman et al., 2005; Bombois

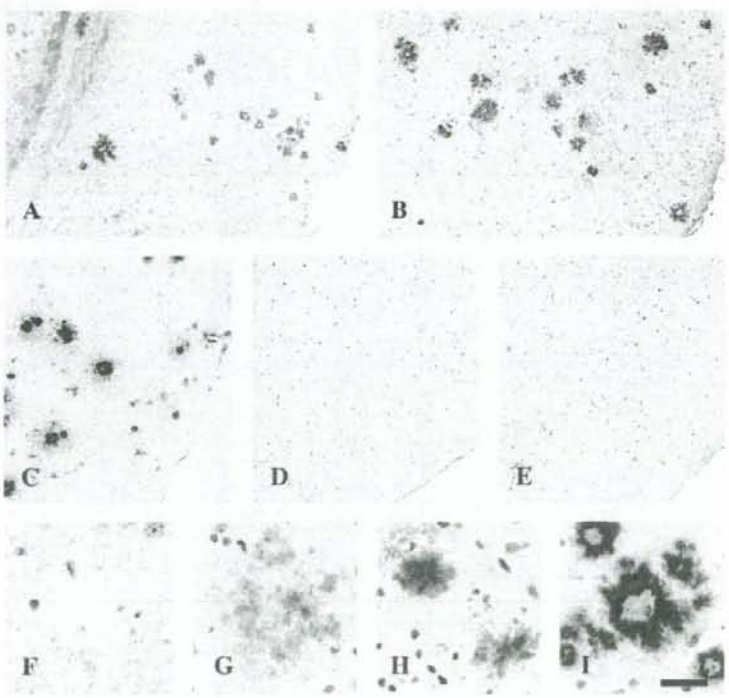

Fig. 1 – TAPIR using plasma and Tg2576 mouse brains. Many senile plaques in Tg2576 brains were labeled prominently in A (AD group, TAPIR grading ++) and B (aNC group, TAPIR grading ++). C: control Aβ immunostaining with Ab9204; no senile plaques were labeled in D (AD group, TAPIR grading –) and E (aNC group TAPIR grading –). F to I are examples of TAPIR grade. F: TAPIR –; G:±; H: +; I: ++. Scale bar=6.25 μm in A–E and 25 μm in F–I.

et al., 2007). Here, we examined 113 AD cases and 155 age-matched normal controls by TAPIR assay in order to clarify the positive rates, antibody characters, correlations with clinical symptoms, and clinical roles of naturally occurring antibodies against β-amyloid plaques. Modification of plasma Aβ40 and Aβ42 concentrations by antibodies to Aβ was also studied based on age- or AD-dependent alterations of plasma Aβ levels.

2. Results

2.1. *High positive TAPIR rate but no difference between AD and aNC groups*

Some plasma samples from AD and aNC groups strongly labeled nearly all amyloid plaque cores (Fig. 1A, B and I; grading ++) as did Ab9201 (Fig. 1C). Other plasma samples from both groups showed negative (Fig. 1D, E, F, grading –), weak (Fig. 1G, grading ±), or positive (Fig. 1H, grading +) labeling. The TAPIR staining was detected by anti-IgG second antibody, but not with anti-IgM or IgA antibodies (not shown), thus TAPIR-positive antibody was shown to be IgG antibody. The specificity of TAPIR-positive antibody was examined by immunoprecipitation of Aβ as described in 2.3. In the AD group, 42 cases (37.2%) were TAPIR –, 20 (17.8%) were ±, 44 (38.9%) were grading +, and 7 (6.2%) were ++. Fifty one of 113 AD patients were ++ and +, suggesting frequent appearance (45.1%) of naturally occurring antibodies to amyloid plaque cores. In the aNC group, 54 cases (34.8%) were TAPIR –, 37 (23.9%) were ±, 44 (28.4%) were +, and 20 (12.9%) were ++. Sixty-four cases of 155 aNC group (41.3%) were TAPIR ++ or +. No significant differences were detected by Mann–Whitney's *U* tests in the positive rates of naturally occurring antibodies to amyloid plaque cores among groups ($p=0.77$), or comparisons between the positive AD group (++ and +), negative AD group (± and –), positive aNC group (++ and +) and negative aNC (± and –) group ($p=0.54$) (Table 1).

2.2. *TAPIR was not correlated with clinical symptoms*

There were no significant differences in gender or mean age in both AD and aNC groups (Table 1). No significant differences were observed in MMS scores and disease duration among the TAPIR –, ±, +, ++ subgroups of AD samples (Table 1 and Fig. 2A, B). There were also no significant differences in the progressive decline of MMS scores among these AD subgroups (Fig. 2C). The presence of naturally occurring antibodies to Aβ as detected by TAPIR may therefore not improve prognosis of AD.

2.3. *TAPIR-positive plasma recognized Aβ40 and FAβ, but Aβ42 very weakly*

As indicated in Fig. 3, freshly prepared Aβ40 and Aβ42 were composed of monomers and dimers. However, formic acid extractable Aβ (FAβ) exhibited polymerization as shown by the higher molecular mass of its oligomers (Fig. 3, left panel). Immunoprecipitation with TAPIR ++/+ plasma obtained from the AD and aNC groups retrieved Aβ40 monomers and dimers as well as higher molecular mass polymers. Immunodetection of monomeric Aβ42 using 6E10 was very weak, whereas no dimeric form of Aβ42 was detected (Fig. 3 right panels). These findings suggest that TAPIR-positive plasma reacts with Aβ, but its reactivity to Aβ42 is very weak.

2.4. *Antibodies to Aβ appeared before Aβ amyloid deposits in the brain*

In order to clarify when these antibodies against Aβ appear, we additionally examined the remaining 50 plasma samples from subjects younger than 43 yeas old in the tNC group. Surprisingly, TAPIR revealed that antibodies to Aβ appeared in a 2 year-old child and also in some young subjects (TAPIR +; Fig. 4A, B and C). TAPIR-positive rates were 57% by 10 years old ($n=7$; 4 TAPIR +), 64% by 20 years old ($n=11$; 6 TAPIR +), 20% by 30 years old ($n=10$; 2 TAPIR +) and 10% by 40 years old ($n=10$; 1 TAPIR +). To confirm further this early appearance of antibodies to Aβ, immunoprecipitation was performed. Essentially identical finding to those seen in the AD and aNC groups were revealed (Fig. 4 D–F). Aβ40 and FAβ monomers and dimers were strongly immunoprecipitated (arrows). However, immunoprecipitation of the Aβ42 monomer was also weak and the Aβ42 dimer was absent in TAPIR-positive plasma from younger controls.

This was also the case in plasma obtained from Tg2576 model mice. Plasma from younger and older Tg2576 mice labeled

Table 1 – Summary of tissue amyloid plaque immunoreactivity (TAPIR) in AD and control groups

	Grade	Cases	rate (%)	Gender (M/F)	Mean age (SD), yr	Mean MMSE (SD)	Mean duration (SD), mo
AD ($n=113$)	–	42	37.2	11/31	75.4 (7.2)	14.7 (7.2)	50.9 (34.4)
	±	20	17.8	5/15	75.0 (8.0)	15.4 (7.3)	39.5 (27.4)
	+	44	38.9	14/30	74.5 (8.2)	14.9 (6.3)	37.5 (24.7)
	++	7	6.2	3/4	77.3 (5.3)	14.7 (6.2)	47.7 (19.7)
aNC ($n=155$)	–	54	34.8	21/33	74.7 (9.5)	29.9 (0.3)	–
	±	37	23.9	16/21	76.0 (8.7)	29.6 (0.5)	–
	+	44	28.4	19/25	77.9 (8.0)	29.7 (0.4)	–
	++	20	12.9	3/17	74.2 (11.8)	29.9 (0.3)	–

In the AD group, 42 cases (37.2%) were TAPIR –, 20 (17.8%) were ±, 44 (38.9%) were +, and 7 (6.2%) were ++; 51 of 113 AD patients were ++ and +, suggesting high rate of TAPIR (45.1%). In the aNC group, 54 cases (34.8%) were TAPIR –, 37 (23.9%) were ±, 44 (28.4%) were +, and 20 (12.9%) were ++; 64 of 155 aNC controls (41.3%) were TAPIR-positive. No significant differences were found in the positive TAPIR rate within each group ($p=0.77$), or in comparisons between the positive AD group (++ and +), negative AD group (± and –), positive aNC group (++ and +), and negative aNC (± and –) group ($p=0.54$). There were no significant differences in gender, mean age, mean MMS score or mean disease duration according to TAPIR grade in both AD and aNC groups. yr: years old; mo: months.

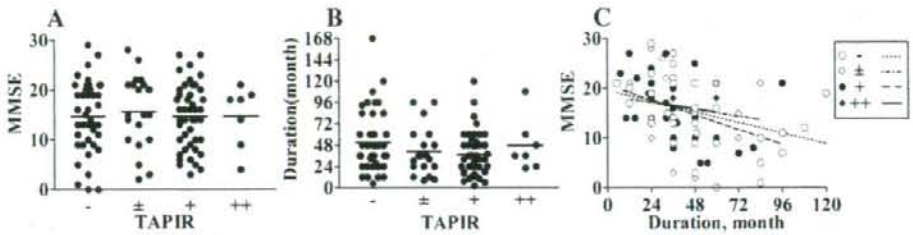

Fig. 2 – TAPIR was not correlated with clinical symptoms. There were no significant differences in MMS scores (A), disease duration (B) or decline of the clinical course of AD according to TAPIR grade. No significant difference in the decline of MMS scores according to duration was shown among AD subgroups (C). Y = −0.09X + 19.54, r^2 = 0.19, p = 0.01 in TAPIR − (○); Y = −0.06X + 18.50, r^2 = 18.50, p = 0.52 in TAPIR ± (◊); Y = 0.12X + 20.59, r^2 = 0.17, p = 0.02 in TAPIR + (●); Y = −0.06X + 18.63, r^2 = 0.04, p = 0.72 in TAPIR ++ (♦).

amyloid cores in AD brains (Fig. 4G–I). The appearance rate was 1/3 at 4 months old (1 TAPIR +), 3/3 at 8 months old (1 TAPIR ++ and 2 TAPIR +), 1/1 at 16 months old (1 TAPIR ++) and 1/1 at 23 months old mice (1 TAPIR +).

Finally, we summarized age-dependent TAPIR-positive rates (TAPIR grading + and ++) in 10 year increments in both AD and tNC groups (Fig. 4J). TAPIR-positive rates were high in young subjects (1–20 years old), low during adulthood (21–50 years old) and then increased again after 50. No differences were observed between AD and tNC samples from 50 to 91 years old. Thus, the appearance of antibodies to Aβ preceded Aβ amyloid deposition in human and model mouse brains.

2.5. *Levels of plasma Aβ40 and Aβ42 were age-dependently regulated in the tNC group*

To examine the effect of antibodies to Aβ on plasma Aβ concentrations, we measured levels of Aβ40 and Aβ42 in 318 plasma samples by specific ELISA. In the tNC group, plasma Aβ40 levels increased after 40 years of age (Fig. 5A; $p < 0.0001$). On the contrary, plasma Aβ42 levels increased between the teens and twenties, then gradually declined with age (Fig. 5B; $p = 0.0158$). The Aβ ratio (Aβ40/Aβ42) was stable until ~30 years old and then gradually increased (Fig. 5C; $p < 0.0001$).

2.6. *Plasma Aβ ratio is increased in AD*

Significantly increased levels of plasma Aβ40 were observed in the AD group (112 ± 39.51 pmol/L) compared to the aNC group (95.38 ± 32.30; $p < 0.0002$; Fig. 5D). Aβ42 levels were significantly decreased in the AD group (10.29 ± 13.80 pmol/L) compared to the aNC group (12.13 ± 12.29; $p < 0.0001$; Fig. 5E). Based on these changes, the Aβ ratio (Aβ40/Aβ42) was more strongly increased in the AD group (14.42 ± 10.00) than in the aNC group (8.34 ± 3.83; $p < 0.0001$; Fig. 5F). ROC analysis of the Aβ ratio indicated that the significant cut off value was 9.0, which provided high sensitivity (78.8%) and low specificity (30.3%) for clinical diagnosis of AD. When the mean + 2 SD (15.9) of the aNC group was used as a cut off value, the sensitivity was 24% and the specificity was 96%. When AD was divided into 3 subgroups according to clinical stage, increasing Aβ40 levels and Aβ ratio, as well as decreasing Aβ42 levels progressed from the early stage to the advanced stage (Fig. 5G–I). Thus, the plasma Aβ ratio can be used as a specific biomarker for AD although the sensitivity and specificity are lower than those of CSF samples (Kanai et al., 1998; Shoji et al., 2001; Shoji, 2002).

2.7. *TAPIR did not modify Aβ concentration*

Finally, we examined whether antibodies to Aβ could affect levels of plasma Aβ40 and Aβ42. There were no significant differences in the concentrations of plasma Aβ40 or Aβ42, or in the Aβ ratio among AD and aNC classified by TAPIR score (Fig. 6A–C).

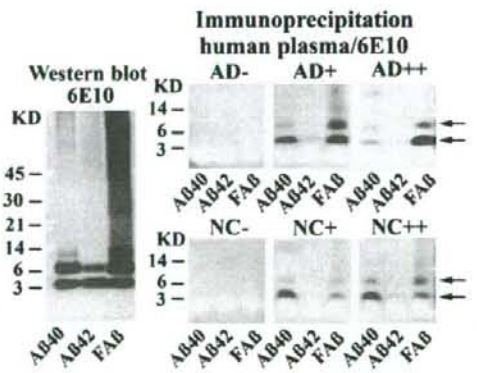

Fig. 3 – TAPIR-positive plasma immunoprecipitated Aβ40 and amyloid Aβ, but Aβ42 very weakly. On direct western blotting of synthetic Aβ40, Aβ42, and FAβ from the AD brain, antibody 6E10 detected monomers and dimers of Aβ40, Aβ42 and brain amyloid Aβ with smear aggregates (left panel). Immunoprecipitations of Aβ40, Aβ42, and FAβ using TAPIR −, +, and ++ plasma from the AD group (right upper panel, AD) or the aNC group (right lower panel, NC) were labeled by antibody 6E10, showing that monomers (arrow) and dimers (arrow) of Aβ40 were recognized by TAPIR-positive plasma (grading + and ++) in addition to Aβ42 monomers, and brain Aβ amyloid monomers and dimers with smear aggregates, which showed weak signals.

3. Discussion

In our study, a high positive rate of TAPIR was found in both AD (45.1%) and aNC (41.2%) groups, but no significant difference was found between these groups. Essentially the same findings were observed even in strongly positive (++) subgroups of AD (6.2%) and aNC (12.9%). Non-parametric analysis revealed that neither MMSE score nor disease duration correlated with TAPIR grade, indicating that the physiological impact of naturally occurring anti-Aβ antibodies is below clinical significance. This is consistent with previous reports describing frequent presence of low levels of antibodies to Aβ40 or Aβ42 peptides as detected by ELISA in plasma and CSF. A large scale study by Hyman et al. showed by ELISA that there were low and modest levels of anti-Aβ42 peptide antibodies in 52.3% and 4.7% of 365 plasma samples from AD and age-matched controls, respectively (Hyman et al., 2001). Neither the presence nor the amounts of anti-Aβ antibodies correlated with the likelihood of developing dementia or plasma levels of Aβ40 and Aβ42 (Hyman et al., 2001; Orgogozo et al., 2003; Moir et al., 2005; Li et al., 2007). Our study indicated that TAPIR-

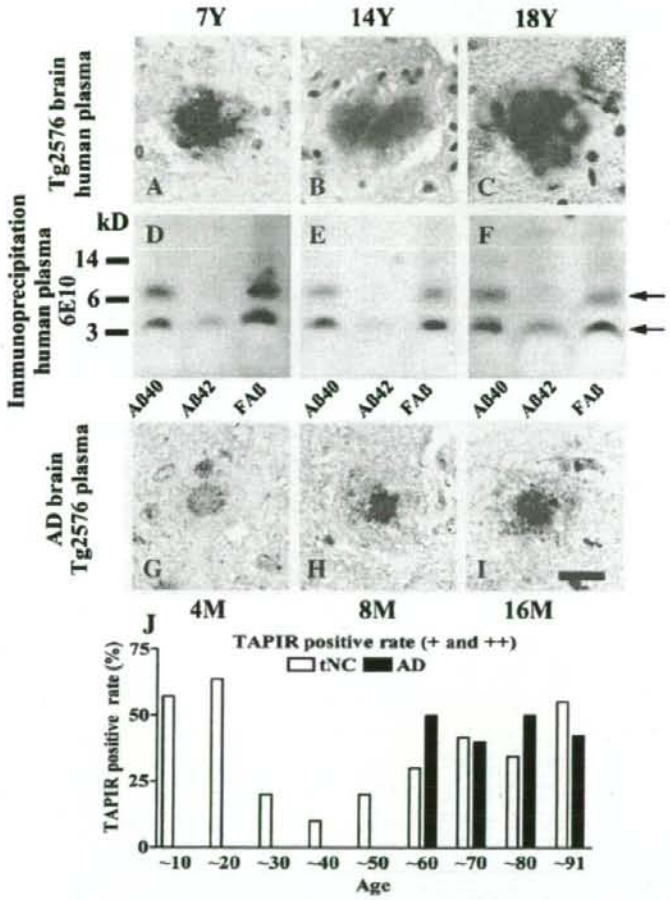

Fig. 4 – Antibodies to Aβ appeared before Aβ amyloid deposits in the brain. TAPIR was positive in 7 years old (TAPIR +; A, 7Y), 14 years old (TAPIR +; B, 14Y), and 18 years old young persons (TAPIR +, C, 18Y). TAPIR-positive plasma strongly immunoprecipitated monomers and dimers (arrow) of Aβ40 and FAβ, and weakly immunoprecipitated monomers of Aβ42 and Aβ amyloid (D, E and F; corresponding plasma of upper panels; D and A 7Y, E and B 14Y and F and C 18Y). Plasma from younger and older Tg2576 mice also labeled amyloid cores in AD brains (G: 4 months old TG; H: 8 months old Tg and I: 16 months old Tg). Bar scale = 15 μm. J: TAPIR-positive rates in the tNC group according to age. Columns show the TAPIR-positive rate (TAPIR grading + and ++) for 10 year increases in the AD (black columns) and tNC (white columns) groups. TAPIR-positive rates were high in young subjects (1–20 years old), low during adulthood (21–50 years old) and then increased again after age 50. No differences were observed between AD and tNC groups in samples from subjects 50 to 91 years old.

positive antibodies to Aβ amyloid plaques also occur naturally and frequently in human plasma and that their titers are not sufficient to prevent development of dementia. High titer of antibodies are necessary to improve the Aβ burden as shown in AD patients treated with an Aβ vaccine (Hock et al., 2002) or an anti-Aβ antibody infusion therapy (Dodel et al., 2002).

TAPIR is a new method to detect anti-Aβ antibodies (Hock et al., 2002, 2003). The fact that cognitive impairment was improved in patients who generated anti-Aβ antibodies after Aβ vaccination leads us to hypothesize that TAPIR-positive anti-Aβ antibodies are substantially different from naturally occurring anti-Aβ peptides antibodies in their specificity for Aβ40 and Aβ42 species or conformational epitopes of Aβ oligomers (Mirra et al., 1991; Kayed et al., 2003). Antibodies labeling Aβ amyloid plaques were more effective for the clearance of the Aβ burden of transgenic mice in passive immunization experiments (Bard et al., 2000). Direct action of the anti-Aβ antibody through the blood–brain barrier without T-cell proliferation as well as microglial clearance via the Fc or non-Fc portion of the antibodies mediated disruption of the plaque structure (Bard et al., 2000; Bacskai et al., 2002; Lombardo et al., 2003). Binding of an IgG2a antibody to the special N-terminal region of Aβ correlated with a clearance response (Bard et al., 2003). Injected antibodies may bind and sequestrate blood Aβ completely and disturb the balance between CSF Aβ and blood Aβ, leading to increased clearance from the brain into the blood (DeMattos et al., 2001; DeMattos et al., 2002). Clearance of diffusible Aβ oligomers that impair cognitive function was considered to be another target for passive immunization (Kayed et al., 2003). Recently a 56-kDa soluble amyloid-β assembly termed Aβ*56 has been shown to disrupt memory (Lesné et al., 2006), and Aβ oligomers have been shown to be increased in CSF from AD patients (Georganopoulou et al., 2005).

These reports all support the hypothesis that naturally occurring TAPIR-positive antibodies to Aβ recognize special Aβ species. Our immunoprecipitation study suggested that

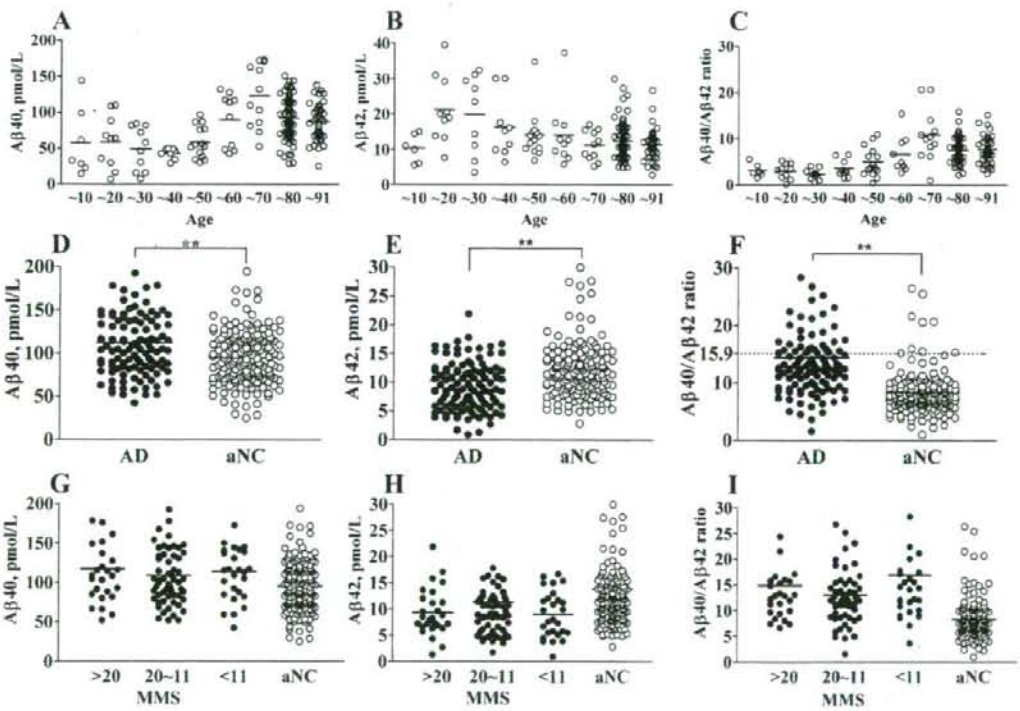

Fig. 5 – Age-dependent regulation of plasma Aβ levels in controls, and their alteration in AD. Plasma Aβ40 and Aβ42 levels showed different age-dependent alterations in the tNC group. Aβ40 levels increased from age 50 and decreased from age 70 (A). Aβ42 levels were high in the teens and twenties, then gradually decreased with age (B). Based on these different changes, the Aβ ratio (Aβ40/Aβ42) progressively increased from age 40 (C). Significantly increased levels of Aβ40 (D: $p=0.0002$) and increased Aβ ratio (F: $p<0.0001$) as well as decreased levels of Aβ42 (E: $p<0.0001$) were shown between the AD and aNC groups. When the mean +2SD of the Aβ ratio in the aNC group was used as a diagnostic marker for AD, the cut off value 15.9 (dot line) provided 24% sensitivity and 96% specificity (F). Constant alterations of plasma Aβ levels in AD were recognized at the early (MMS score >20), moderate (MMS score 20–11), and advanced stages (MMS score <11) (G–I). A, D, G: Aβ40; B, E, H: Aβ42; C, F, I: Aβ ratio. Bars show mean levels.

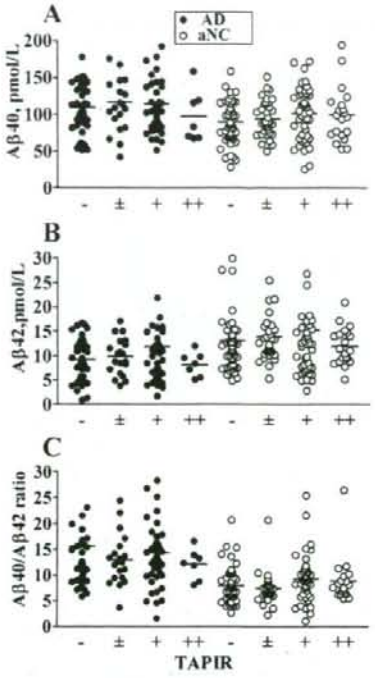

Fig. 6 – TAPIR did not modify Aβ concentration. No significant differences were found in Aβ40 and Aβ42 concentrations as well as Aβ ratios among all TAPIR grades (–, ±, + and ++) in AD (•) and aNC (○) group (A, B and C).

TAPIR ++/+ plasma obtained from AD and aNC subjects retrieved Aβ40 monomers and dimers as well as higher molecular mass polymers. Immunodetection of monomeric Aβ42 using 6E10 was very weak, whereas no dimeric form of Aβ42 was detected under our testing conditions. The absence of anti-Aβ42 dimer antibodies and the relatively low levels of anti-Aβ42 monomers were characteristic of naturally occurring antibodies to Aβ. These findings are considered to be another reason why naturally occurring antibodies to Aβ are not sufficient for prevention of development of dementia.

Our TAPIR assay also showed that anti-Aβ antibodies were naturally present throughout the entire human life span. It is relevant to note that naturally occurring anti-Aβ antibodies were unequivocally detected in young human subjects as well as young Tg2576 mice. In relative terms, the positive rates of anti-Aβ antibodies were highest in young individuals, lowest in those middle-aged and higher in the elderly. The presence of anti-Aβ antibodies in young human subjects was characterized by the subsequent immunoprecipitation study. Anti-Aβ antibodies retrieved Aβ40 monomers and dimers as well as high molecular mass oligomers in FAβ fractions, but they retrieved fewer Aβ42 dimers. To our knowledge, this is the first report showing the relatively selective presence of anti-Aβ40 antibodies, and reduced amounts of anti-Aβ42 antibodies in young individuals. We also found that this was the case in normal elderly as well as AD patients, suggesting that the immune response to Aβ was unchanged in the two groups tested. Impaired spontaneous production of anti-Aβ42 antibodies also took place in elderly human subjects as well as AD patients. It is unknown why these antibodies to Aβ appeared more frequently in the young and the elderly populations and how specific immune tolerance for Aβ42 monomers and oligomers could be present. However, it should be noted that naturally occurring antibodies to Aβ appear in young human subjects and young Tg2576 mice, which do not develop an Aβ burden in their brain. The appearance of naturally occurring antibodies to Aβ is not correlated with the Aβ burden in the brain.

The exact mechanism underlying spontaneous anti-Aβ antibody production remains unknown. Although increased Aβ42 levels have been detected in transgenic animal models (Kawarabayashi et al., 2001), immune hyporesponsiveness to Aβ42 was also shown (Monsonego et al., 2001). Increased T-cell reactivity to Aβ42 was shown to increase in elderly individuals and patients with AD (Monsonego et al., 2003). However, the previous findings and our results could not show increased titers of anti-Aβ42 antibodies in these groups. Thus, hyopoimmunue responses to Aβ42, especially to the Aβ42 oligomer, actually occurred in AD and healthy populations. Since Aβ42 is highly pathogenic and neurotoxic, Aβ42 may be sequestered and spontaneous immune responses to Aβ may be suppressed in human populations. For effective immunotherapy as shown in transgenic mice studies and Aβ vaccine trials (Orgogozo et al., 2003; Hock et al., 2003), it is necessary to further generate antibodies to Aβ42 oligomers as well as monomers and monitor their titers. Furthermore, in order to prevent unexpected adverse reaction as seen in the Phase II trials of AN1792, detection of these spontaneous antibodies to Aβ will be necessary before treatment.

Recent studies have shown that plasma concentrations of Aβ40 and Aβ42 are possible biomarkers (Ertekin-Taner et al., 2000; Fukumoto et al., 2003; Mayeux et al., 1999, 2003; van Oijen et al., 2006; Graff-Radford et al., 2007) and can be used to monitor the effects of special treatments for AD (Dodel et al., 2002; DeMattos et al., 2001, 2002). After administration of an antibody to Aβ, the rapid increase in plasma Aβ was highly correlated with the amyloid burden in the brain (DeMattos et al., 2002), suggesting the possibility that naturally occurring anti-Aβ antibodies may cause increases the plasma Aβ concentration. In order to clarify this effect, we first analyzed age-dependent levels of plasma Aβ40 and Aβ42, and then examined alterations of Aβ40 and Aβ42 levels according to the presence or absence of AD and antibodies to Aβ. In the tNC group, plasma Aβ40 levels increased from age 40. Plasma Aβ42 levels increased between age 10 and 20, then gradually declined with age. The Aβ ratio (Aβ40/Aβ42) was stable until about 30 years and then gradually increased. These natural time courses were identical to those of CSF Aβ40 levels, but completely different from those of CSF Aβ42 levels. CSF levels of Aβ40 and Aβ42 showed U-shaped age-dependent curves, suggesting their correlation with brain development and decline (Kanai et al., 1998; Shoji et al., 2001; Shoji, 2002). The correlation was prominent between the appearance of naturally occurring anti-Aβ antibodies and increased Aβ40 levels in

the CSF and plasma. Increased opportunities for immunological exposure to Aβ40 monomers and oligomers in immature or declining brains in young and elderly indivisuals may be sources for the naturally occurring immune response to Aβ40.

Based on these natural time courses of plasma Aβ concentrations, a comparison between AD and aNC groups was performed that provided intriguing findings. Significantly increased levels of plasma Aβ40, increased Aβ ratio and decreased levels of Aβ42 were revealed in the AD group when compared to the aNC group. Since a clear separation was obtained in the Aβ ratio between the AD and aNC groups, we evaluated the value of the Aβ ratio as a diagnostic or monitor maker of AD. ROC analysis indicated high sensitivity (78.8%) and low specificity (30.3%) for diagnosis of AD. When the mean+2 SD (15.9) of the aNC group was used as a cut off value, the sensitivity was 24% and specificity was 96%. When AD was divided into 3 groups according to clinical stage, the Aβ ratio increased progressively from the early stage to the advanced stages of AD. These findings show that plasma Aβ ratio can be used as an easy, non-invasive, and useful biomarker for diagnosis and monitoring of clinical symptoms of AD, although the sensitivity and specificity are lower than those in CSF samples (Kanai et al., 1998; Shoji et al., 2001; Shoji, 2002). However, naturally occurring antibodies to Aβ did not affect plasma Aβ40 or Aβ42 levels, or the Aβ ratio. There was a possibility that our ELISA system could not detect increased levels of Aβ40 and Aβ42 oligomers. However, all results taken together, suggest that the titer and specificity of naturally occurring anti-Aβ antibodies were not sufficient to elevate plasma Aβ concentrations and increase Aβ clearance from the brain to the peripheral blood with subsequent improvement of clinical symptoms. Higher titers of antibodies to Aβ42 oligomers will likely be necessary to facilitate Aβ clearance from brain amyloid to peripheral blood for AD treatment.

4. Experimental procedures

4.1. *Patients and normal controls*

After informed consent was given, blood samples were collected into 0.1% EDTA from a total of 318 subjects including 113 patients with AD (AD group) and 205 normal controls (total normal control group: tNC group). As age-matched controls (aNC group), 115 samples from subjects over 43 years old were selected from the tNC group. The basic findings for the respective groups are summarized in Table 2. The clinical diagnosis of AD was based on NINCDS–ADRDA criteria (McKhann et al., 1984). Appropriate diagnostic studies including magnetic resonance imaging and single photon emission computed tomography were used to exclude other disorders of dementia. The clinical severity of AD was evaluated using the Mini-Mental State Examination (MMS) (Folstein et al., 1975). AD patients were divided into 3 subgroups according to clinical stages: early stage MMS score >20, moderate stage MMS score 10–20, advanced stage MMS score <10. Controls were judged to be normal based on their MMS score (>28 points) and follow-up with neurological evaluation. After separation of plasma from blood cells, plasma was stored frozen at −80 °C until use.

Table 2 – Summary of the study subjects

	No. of subjects	Gender (M/F)	Mean age (range), yr	Mean MMS Score (SD)	Mean duration (SD), mo
AD	113	32/81	75 (55–89)	14.9 (6.7)	44 (28)
tNC	205	84/121	64 (1–91)	29.8 (0.3)	–
aNC	155	59/96	76 (43–91)	29.7 (0.4)	–
Total	318	116/202	68 (1–91)		

AD: Alzheimer's disease patients; tNC: total normal controls; aNC: age-matched controls over 43 years old selected from the tNC group; M/F: male and female; yr: years old; MMS: Mini-Mental State Examination; SD: standard deviation; Duration: duration from onset, mo months.

4.2. *Tissue amyloid plaque immunoreactivity (TAPIR)*

Five micrometers serial paraffin sections of brains from Tg2576 mice (16–18 months old) or Alzheimer's patients were used. Sections were immersed in 0.5% periodic acid for blocking intrinsic peroxidase and treated with 99% formic acid for 3 min to increase Aβ staining. Sections were then immersed with blocking solution with 5% normal serum in 50 mM phosphate-buffered saline (PBS) containing 0.05% Tween20 and 4% Block Ace (Snow Brand Milk Products, Saporo, Japan) for 1 h; goat serum was used to stain human plasma, and horse serum was used to stain mouse plasma. Sections were incubated at 4 °C overnight with human or mouse plasma diluted with blocking solution (1:100). Sections were then incubated with biotinyzed second antibody (anti-human goat antibody or anti-mouse horse antibody), and horseradish peroxidase-conjugated avidin–biotin complex of Vectastain Elite ABC kit (Vector, Burlingame, CA). Immunoreactivity was visualized by incubation with 0.03% 3, 3′-diaminobenzidine, and 0.02% H_2O_2. Tissue sections were counterstained with hematoxylin. Immunostaining with Ab9204 (Saido et al., 1995) (1:1000, antibody to a synthetic Aβ peptide starting from the amino-terminus of normal L-aspartate) or without the primary antibody were used as positive and negative controls, respectively.

4.3. *Grading of TAPIR*

TAPIR findings were classified into 4 levels: negative −, no senile plaque core (Fig. 1F); weakly positive ±, senile plaque cores were stained weakly and less than 5 cores were stained in each brain section on a slide (Fig. 1G); positive +, ≥5 senile plaque cores were stained clearly in at least one brain section per slide (Fig. 1H); strongly positive ++, most senile plaque cores were strongly labeled when compared to Ab9204 immunostaining (Fig. 1I). Immunostaining findings of diffuse plaques, amyloid angiopathy, positive neurons, degenerative neurites and glial cells were excluded from this grading.

4.4. *Purification of amyloid Aβ (FAβ)*

An autopsy brain fulfilling the CERAD criteria for definite AD (Mirra et al., 1991) was selected. About 2 g of gray matter of the AD brain was homogenized with 4 volumes of TBS (10 mM Tris, 150 mM NaCl, pH 8) with protease inhibitors (1 μg/ml

Leupeptin, 1 μg/ml TLCK, 0.1 μg/ml Pepstain A, 1 mM phenylmethysulfonyl fluoride and 1 mM EDTA), and centrifuged at 100,000 ×g for 1 h. The resulting pellet was extracted with 10 ml of 10% sodium dodecyl sulfate (SDS) in TBS and then with 1 ml of 99% formic acid (FA). The final supernatant was lyophilized, dissolved with 20 μl of 99% dimethylsulfoxide (DMSO), and stored at −80 °C until use (formic acid soluble amyloid Aβ fraction: FAβ) (Harigaya et al., 1995; Matsubara et al., 1999).

4.5. *Immunoprecipation*

20 μl of protein G agarose (Roche diagnostic GmbH, Germany) was washed 3 times with 1 ml RIPA buffer (50 mM Tris, 1% Triton X-100, 0.1% SDS, 0.5% cholic acid and 150 mM NaCl, pH 8.0). Prewashed protein G agarose was mixed with 600 ng synthetic Aβ40, 600 ng synthetic Aβ42 (Sigma, Mo) or 300 ng FAβ in 1 ml of RIPA buffer and incubated at room temperature for 30 min. After centrifugation, the resulting supernatant was mixed again with 20 μl of prewashed protein G agarose and 10 μl of plasma, incubated at room temperature for 3 h, and then centrifuged. The pellet was boiled with 1× NuPage LDS sample buffer containing 0.1 M dithiothreitol for 10 min at 70 °C and separated on a 4 to 12% NuPage Bis–Tris gel (Invitrogen, CA). After electro-transfer, the blot membrane was blocked with 10% skim milk (Snow Brand Milk Products, Saporo, Japan) in TBS with 0.05% Tween 20 (TBST), and incubated with monoclonal 6E10 (specific to Aβ1-16, 1:1000, Signet Lab. Inc. MA) at 4 °C overnight. After washing and incubation with horseradish-peroxidase-conjugated goat anti-mouse IgG (1:2000, Amersham Biosci, Buckinghamshire, UK) at RT for 2 h, the signal was developed by SuperSignal west Dura extended duration substrate (Pierce Biotechology, CA), and quantified by a luminoimage analyzer (LAS 1000-mini, Fuji film, Japan).

4.6. *Quantification of plasma Aβ40 and Aβ42 concentrations by ELISA*

Sandwich ELISA was used to specifically quantify whole plasma Aβ, as previously described (Matsubara et al., 1999). Microplates were pre-coated with monoclonal BNT77 (IgA, anti-Aβ11-28, specific Aβ11-16) and sequentially incubated with 100 μl of samples followed by horseradish-peroxidase-conjugated BA27 (anti-Aβ1-40, specific Aβ40) or BC05 (anti-Aβ35-43, specific Aβ42 and Aβ43) (Kawarabayashi et al., 2001). Synthetic Aβ40 (peptide content: 79.95%, Sigma, MO) and Aβ42 (peptide content:76.58%, Sigma, MO) were used for standard Aβ. The sensitivity was 40 fmol/ml in the Aβ40 assay and 10 fmol/ml in the Aβ42 assay. Both intra-assay coefficients of variation were less than 10% (Matsubara et al., 1999).

4.7. *Statistical analysis*

Comparisons among the groups using Student's *t*-test, one-way analysis of variance or a non-parametric test with post hoc tests, a receiver-operating characteristic (ROC) curve analysis to determine the cut off value, Mann–Whitney *U* test for appearance rates, and 1st order regression analysis of the relationship between MMS score and AD duration were all performed using SPSS 11.0 (SSPS Inc., IL) and GraphPad Prism, Version 4 (GraphPad Software, San Diego, CA).

Acknowledgments

We thank Yasuko Nogami and Hisae Narihiro for technical assistance, and Dr. TC Saido for kind gift of Ab9204. All animal experiments were performed according to guidelines established in the "Guide for the Care and Use of Laboratory Animals". This study was performed with permission of the ethical committee of Okayama University. Supported by a Grant-in-Aid from the Grants-in-Aid for Primary Amyloidosis Research Committee (M.S.), of the Ministry of Health, Labor and Welfare of Japan and by Grants-in-Aid for Scientific Research (B) (M.S.: 19390233, K.A.: 18390257), (C) (M.I.: 19590980, T.K.: 19590976, A.S.: 18500276, E.M.: 18590968), from the Ministry of Education, Culture, Sports, Science and Technology, Japan.

REFERENCES

Bacskai, B.J., Kajdasz, S.T., McLellan, M.E., Games, D., Seubert, P., Schenk, D., Hyman, B.T., 2002. Non-Fc-mediated mechanisms are involved in clearance of amyloid-β in vivo by immunotherapy. J. Neurosci. 22, 7873–7878.

Bard, F., Cannon, C., Barbour, R., Burke, R.L., Games, D., Grajeda, H., Guido, T., Hu, K., Huang, J., Johnson-Wood, K., Khan, K., Kholodenko, D., Lee, M., Lieberburg, I., Motter, R., Nguyen, M., Soriano, F., Vasquez, N., Weiss, K., Welch, B., Seubert, P., Schenk, D., Yednock, T., 2000. Peripherally administered antibodies against amyloid β-peptide enter the central nervous system and reduce pathology in a mouse model of Alzheimer disease. Nat. Med. 6, 916–919.

Bard, F., Barbour, R., Cannon, C., Carretto, R., Fox, M., Games, D., Guido, T., Hoenow, K., Hu, K., Johnson-Wood, K., Khan, K., Kholodenko, D., Lee, C., Lee, M., Motter, R., Nguyen, M., Reed, A., Schenk, D., Tang, P., Vasquez, N., Seubert, P., Yednock, T., 2003. Epitope and isotype specificities of antibodies to β-amyloid peptide for protection against Alzheimer's disease-like neuropathology. Proc. Natl. Acad. Sci. U. S. A. 100, 2023–2038.

Baril, L., Nicolas, L., Croisile, B., Crozier, P., Hessler, C., Sassolas, A., McCormick, J.B., Trannoy, E., 2004. Immune response to Aβ-peptides in peripheral blood from patients with Alzheimer's disease and control subjects. Neurosci. Lett. 355, 226–230.

Bombois, S., Maurage, C.A., Gompel, M., Deramecourt, V., Mackowiak-Cordoliani, M.A., Black, R.S., Lavielle, R., Delacourte, A., Pasquier, F., 2007. Absence of β-amyloid deposits after immunization in Alzheimer disease with Lewy body dementia. Arch. Neurol. 64, 583–587.

DeMattos, R.B., Bales, K.R., Cummins, D.J., Dodart, J.C., Paul, S.M., Holtzman, D.M., 2001. Peripheral anti-Aβ antibody alters CNS and plasma Aβ clearance and decreases brain Aβ burden in a mouse model of Alzheimer's disease. Proc. Natl. Acad. Sci. U. S. A. 98, 8850–8855.

DeMattos, R.B., Bales, K.R., Cummins, D.J., Paul, S.M., Holtzman, D.M., 2002. Brain to plasma amyloid-β efflux: a measure of brain amyloid burden in a mouse model of Alzheimer's disease. Science 295, 2264–2267.

Dodel, R., Hampel, H., Depboylu, C., Lin, S., Gao, F., Schock, S., Jackel, S., Wei, X., Buerger, K., Hoft, C., Hemmer, B., Moller, H.J., Farlow, M., Oertel, W.H., Sommer, N., Du, Y., 2002. Human antibodies against amyloid β peptide: a potential treatment for Alzheimer's disease. Ann. Neurol. 52, 253–256.

Du, Y., Dodel, R., Hampel, H., Buerger, K., Lin, S., Eastwood, B., Bales, K., Gao, F., Moeller, H.J., Oertel, W., Farlow, M., Paul, S.,